Three dimensional surface texture analysis for characterisation of enamel erosion

Austin, Rupert

Awarding institution:
King's College London

Title: Three dimensional surface texture analysis for characterisation of enamel erosion

Author: Rupert Austin

KING'S COLLEGE LONDON DENTAL INSTITUTE AT
GUY'S, KING'S COLLEGE AND ST. THOMAS' HOSPITALS

Three dimensional surface texture analysis for characterisation of enamel erosion

---

Submitted in partial fulfilment of the requirements for the Degree of Master of Science in Prosthodontics

Dr. Rupert S. Austin

BDS (Hons) PhD MJDF RCS Eng MAcMEd AHEA

Department of Fixed and Removable Prosthodontics
King's College London Dental Institute
London SE1 9RT
United Kingdom

September 2013

Abstract

3D surface texture parameters have yet to be applied to dental erosion of human enamel. This project aimed to investigate the effect of acid-mediated erosive enamel wear on the micro-texture of polished (Group 1) and unpolished (Group 2) human enamel *in vitro*. 20 polished and 20 unpolished enamel samples were prepared and subjected to a citric acid erosion and pooled human saliva remineralisation model. For the polished samples, enamel surface microhardness was measured using a Knoop hardness tester, step height enamel loss was measured using a white-light confocal profilometer and surface texture was measured using confocal laser scanning microscopy in combination with MountainsMap® surface analysis software. For the unpolished samples, only surface texture was measured. Statistical analyses were carried out with repeated measures one-way ANOVA. For the polished samples, the microhardness and profilometry confirmed that an early enamel erosion lesion was formed which was then subsequently completely remineralised. The height and functional surface texture parameters were able to successfully characterise the enamel erosion and remineralisation for the polished enamel samples ($P<0.005$) but not for the unpolished enamel samples ($P>0.05$). In conclusion, ISO 25178 3D height and functional surface texture parameters can be used to characterise the effect of enamel demineralisation by acid erosion and enamel remineralisation by human saliva, with reference to established methods for measuring tooth wear (surface microhardness and non-contacting profilometry), in very early enamel erosion lesions in polished enamel surfaces i*n vitro*. This has relevance both for better characterising and understanding the fundamental mechanisms involved in erosive wear of human enamel and also for developing targets for studies investigating the potential effectiveness of surface treatments in enamel erosion, such as oral care products and remineralising surface treatments.

Acknowledgements

I would like to express my deep gratitude to Professor David Bartlett and Dr. Rebecca Moazzez, my research supervisors, for their patient guidance, enthusiastic encouragement and useful critiques of this research work, not to mention their consistently generous support over the past five years of my academic career. Their contributions are hugely appreciated. I would also like to specifically acknowledge Professor Bartlett, Dr. Moazzez and Professor Timothy Watson's valuable and constructive suggestions during the application for the Academy of Medical Sciences Starter Grant.

My grateful thanks are also extended to Mr. Claudiu Giusca for his help and collaboration in the surface texture analysis; Mr. Chrysovalantis Koutsoumourakis who collected the saliva used in this study and Dr. Hande Sar Sankali for her help in the sample preparation.

I would also like to extend my thanks to the laboratory technicians of the Biomaterials department, Mr Peter Pilecki and Mr. Richard Mallett, for their kind help and resourceful efforts which were always made readily available to me throughout this study.

I would like to thank Sheila and Michael, Ismay, Rowena and Geoffrey for their support throughout this project.

Finally, to Deborah, whose love, perseverance and wisdom make it all worthwhile.

Declaration on plagiarism

I, the undersigned, confirm that I have read and understood the statement about plagiarism which is outlined in the course handbook.

I testify that the work that I have submitted accompanying this sheet is wholly my own, and that any quotations or section of text taken from the published or unpublished work of any other person is duly and fully acknowledged therein.

Signed: 

Date submitted: 31st July 2013

Declaration of funding

This project was supported by an award from the Academy of Medical Sciences Starter Grant for Clinical Lecturers Scheme which is funded by Academy of Medical Sciences, The Wellcome Trust, The British Heart Foundation and Arthritis Research UK.

Table of Contents

Review of the literature

1.1. Tooth wear

Tooth wear is the irreversible loss of dental hard tissues from non-bacterial and non-traumatic processes known as dental erosion, attrition and abrasion (Bartlett and Smith 2000). This dental terminology differs from that of materials science, where erosion is viewed as wear caused by flow of fluid with abrasive particles and “corrosion” is a physicochemical or electrochemical process (Isecke, Schütze et al. 2011). Hence some dental researchers also refer to dental erosion as “corrosive wear” and only use tooth wear to refer to mechanical wear from attrition and abrasion (Bartlett, Phillips et al. 1999).

In the current International Classification of Diseases , as shown in Table 1 below, the World Health Organisation classifies the three processes as separate disease entities under Chapter XI / Diseases of the digestive system / Diseases of oral cavity / salivary glands and jaws / Other diseases of hard tissues of teeth (World Health Organisation 1992).

Table 1 The World Health Organisation application of the international classification of diseases to tooth wear (erosion, attrition and abrasion).

K03.0 **Excessive attrition of teeth**	**K03.1** **Abrasion of teeth**	**K03.2** **Erosion of teeth**
Wear:	Due to:	Due to:
approximal	dentifrice	diet
occlusal	habitual	drugs and medicaments
	occupational	persistent vomiting
	ritual	idiopathic
	traditional	occupational
	Wedge defect Not otherwise specified	Not otherwise specified

However, as will be discussed below, these processes should not be considered as independent diseases but rather as synergistic contributors to a multi-factorial disease entity: tooth wear.

1.1.1 Epidemiology

Although tooth wear occurs more in the elderly, both children and young adults are affected with increasing frequency and severity (van't Spijker, Rodriguez et al. 2009; Kreulen, Van't Spijker et al. 2010; The Information Centre for Health and Social Care 2011). In the UK, the prevalence of tooth wear is increasing (especially in young adults) with currently 76 % of adults having some degree of tooth wear and 15 % of young adults having moderate tooth wear (The Information Centre for Health and Social Care 2011). Although severe tooth wear remains rare, when it does occur, as seen

in Figure 3 below it can be very debilitating and challenging to manage, especially when affecting younger people.

1.1.2 Aetiology

There are three main causes of tooth wear: erosion, attrition and abrasion, which act synergistically to destroy enamel and dentine.

Dental erosion is defined as a chemical process that involves the dissolution of enamel and dentine by acids, not derived from bacteria, when the surrounding aqueous phase is under saturated with tooth mineral (Larsen 1990). Dental erosion therefore is chemical loss of tooth minerals as a result of extrinsic (e.g. dietary) acids or intrinsic (i.e. regurgitated from stomach) acids acting on the surface of enamel and dentine.

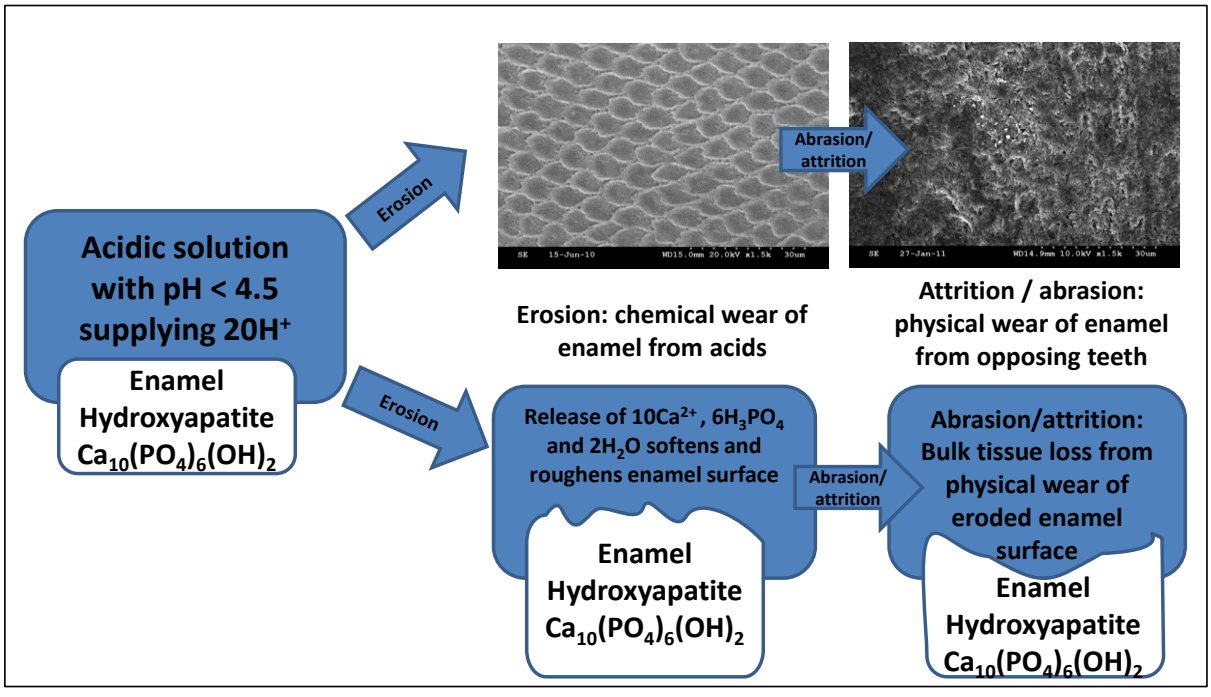

Figure 1 Illustration of the synergistic action of erosion, attrition and abrasion to result in tooth wear at the histological level

In contrast to caries, which develops as subsurface lesion body, dental erosion has been most commonly described as a surface phenomenon (Larsen 1990). Although some authors also believe

that there are subsurface effects, this is somewhat controversial (Featherstone and Lussi 2006). Despite the clinical manifestation of loss of structural integrity and mechanical strength being characterised by smoothness of the tooth surface, as shown in Figure 1 above, the initially histological effects of acid erosion are enamel mineral loss, which results in surface softening and roughening, without bulk tissue loss. If this process continues, the initial softening and roughening is followed by continuous layer-by-layer dissolution of enamel crystals, leading to a permanent loss of tooth volume with a softened layer at the surface of the remaining tissue (Lussi, Schlueter et al. 2011).

This fragile surface is then prone to mechanical wear from attrition or abrasion. Attrition is physical wear as a result of the action of antagonistic teeth removing the demineralised and softened tooth tissue. Abrasion is physical wear as a result of mechanical processes involving foreign bodies, such as tooth brushing, oral soft tissues and food during mastication wearing eroded tooth tissue. In dentine, acids demineralise the inorganic component which activates metallo matrixproteinases thus leading to degradation of the exposed collagenous component of the dentine and resulting in bulk tissue loss.

Chemical, biological and behavioural factors all interact to modify these processes in the oral environment, as shown in Figure 2 below. For example, factors such as saliva quality and quantity, pellicle composition, calcium and phosphate content of food and drinks, fluoride content of oral care products all interact to either promote protection or expedite destruction of the enamel and dentine.

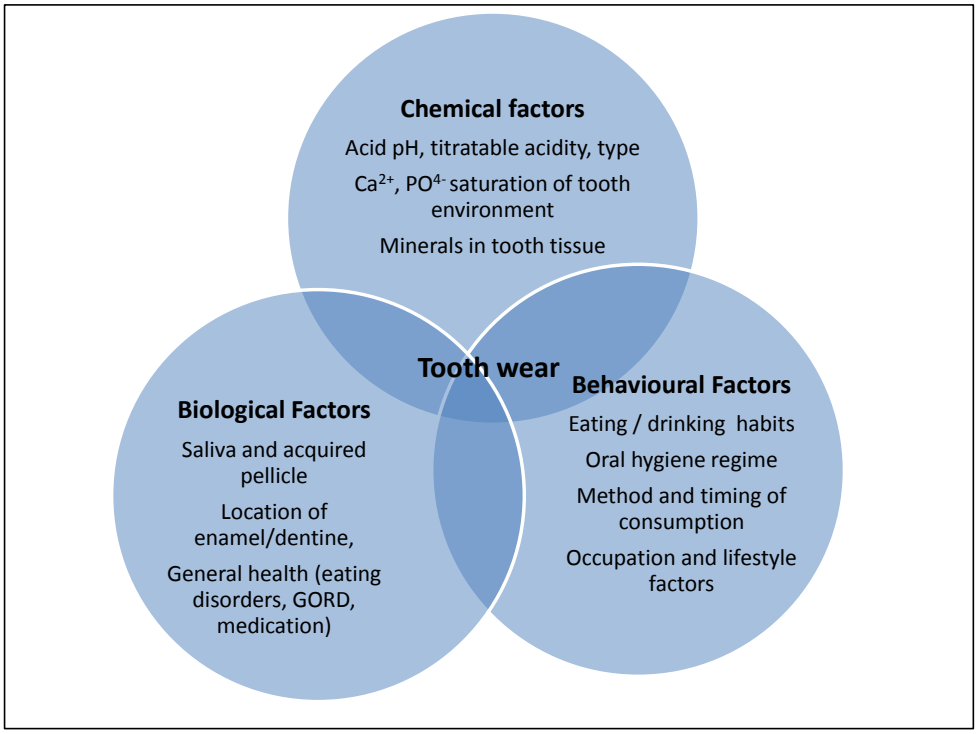

Figure 2 Interplay between chemical, biological and behaviour factors in the development and progression of tooth wear (modified from Magalhães et al 2009)

1.1.3 Clinical features

Clinically, erosive tooth wear appears as smooth silky-shining glazed surfaces with distinct cupping occlusally and restorations appear to rise above the level of the adjacent tooth surface; in cases of more advanced tooth wear, the whole surface is affected and dentine may be exposed (Figure 3) (Lussi 2011).

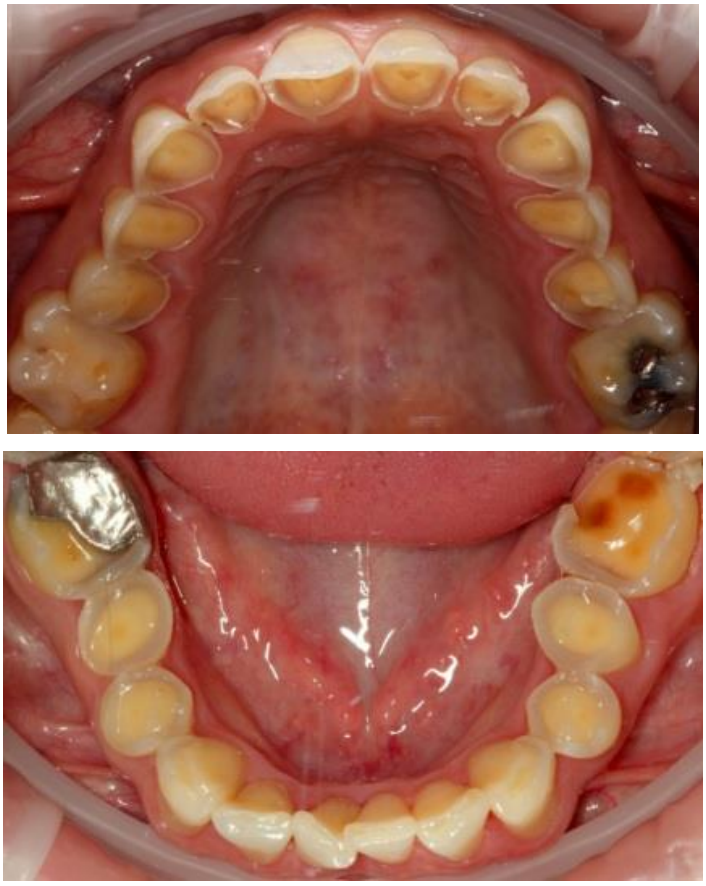

Figure 3 Clinical features of severe tooth wear in a 30 year old male patient

1.1.4 Management

Effective prevention of tooth wear is paramount to protect enamel and dentine before aesthetic or functional concerns negatively impact oral health related quality of life (Al-Omiri, Lamey et al. 2006; Bomfim 2010). Complex and costly restorative dentistry can improve aesthetics if prevention fails, however the restoration of missing tooth tissue with restorative dental materials will not address the causes of the disease.

The first step in management of tooth wear, therefore, is further investigation to include dietary analysis using a diet diary. This may reveal frequency of consumption of acid drinks (soft drinks, fruit juices, sport drinks) and foods (citrus fruits, salad dressing). Medical history questioning may reveal gastrointestinal diseases (esp. gastro-oesophageal reflux disease), eating disorders (esp. anorexia nervosa and bulimia nervosa); alcohol abuse. Many systemic diseases affect salivary flow rate

including diseases of the salivary glands, radiation of the head and neck region, Sjögrens syndrome, diabetes mellitus and chronic renal failure. Medications may be erosive (acetylsalicylic acid, vitamin C) or affect saliva flow rate. These include medications such as antidepressants, anticholinergics, antihistamines, antiemetics, Parkinson medications, as well as recreational drug abuse. Other risk factors include excessively frequent, prolonged or forceful tooth brushing as well as the use of acidic toothpastes or those with a high REA/RDA value. Oral habits can exacerbate effects of erosion, including brushing soon after acid intake; brushing soon after vomiting; acid intakes last thing at night and retaining acid drinks in mouth before swallowing (i.e. frothing, sluicing, sipping, ruminating) (O'Sullivan and Milosevic 2007).

Once the relevant risk factors have been elucidated, the primary aims of management are either to eliminate their occurrence or to mitigate their negative effects through preventative measures, as outlined in Table 2 below.

Table 2 Aims and recommendations for prevention and management of tooth wear (modified from Magalhães et al 2009)

Aim of management	Recommendations
Reduction of extrinsic acid exposure (e.g. diet)	• Reduction of the intake of acidic drinks and snacks • Acidic beverages should be drunk quickly and cooled • Consumption of acidic drinks with a high content of calcium, phosphate, fluoride and xylitol
Reduction of intrinsic acid exposure (stomach acid)	• Evaluation of the etiology of acid exposure, therapy of organic (e.g. reflux, xerostomia) or psychological (e.g. bulimia nervosa) disorders
Reduction of demineralization, enhancement of remineralization	• Increase salivary flow (Chewing sugar-free gum or patients with xerostomia: use of saliva substitutes or systemic medication (cholinergic drugs)) • Behavior after acid contact (Rinsing of the oral cavity with water, milk or low concentrated fluoride solutions; Consumptions of neutralizing food (cheese, milk) • Frequent fluoridation (Use of fluoridated toothpaste, solution and gel)
Reduction of abrasion and attrition	• No tooth brushing immediately after acid consumption • Use of manual toothbrushes or electric toothbrushes applied with gentle pressure • Use of fluoridated toothpastes with low REA/RDA-value • Reduction of grinding and parafunctional activity

1.2. Tooth wear measurement

1.2.1. Clinical measurement using indices

The mainstay of clinical diagnosis is clinical examination and visual assessment of worn surfaces, possibly in combination with a clinical index (O'Sullivan and Milosevic 2007). The basic erosive wear examination (BEWE) assessment is a screening tool which outlines 4 grades of risk according to cumulative score, having examined the whole dentition and scoring each sextant by the worst clinical presentation of the tooth wear in each sextant. (Bartlett, Ganss et al. 2008). The clinical appearance of each grade is listed in Table 3 below.

Table 3 BEWE scoring criteria (Bartlett, Ganss et al. 2008)

Score	Clinical Features
0	No erosive tooth wear
1	Initial loss of surface texture
2*	Distinct defect, hard tissue loss <50% of the surface area
3*	Hard tissue loss ≥50% of the surface area

One of the main strengths of the BEWE is that it can be used in combination with other examination tools, which include study models or photographs. Sensibility testing, study models and intra-oral photographs all aid diagnosis, however studies investigating the use of the BEWE outline issues with recording the earliest signs of tooth wear (Dixon, Sharif et al. 2012) which the BEWE states as “initial loss of surface texture”. A contributing factor to this may well be that the clinical measurement of “initial loss of surface texture” is an outcome that has yet to be clearly defined and to date has not been quantitatively assessed in great detail.

1.2.2. Surface texture measurement of worn human enamel

A surface is defined as 'the outermost part of a material body, considered with respect to its form, texture, or extent' (Oxford English Dictionary 2010). However as is seen in Appendix 1 'A glossary of general terms used in surface texture analysis', for surface texture measurement it is necessary to differentiate between the real surface as perceived with the human senses of touch and sight and the 3D data derived from surface metrology instrumentation (International Organisation of Standardization 1997).

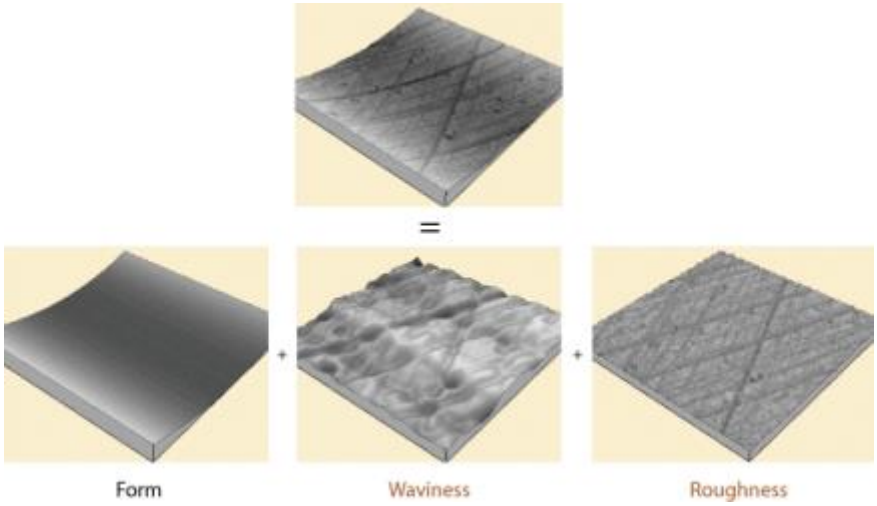

Figure 4 Illustration of how the components of a surface measurement output can be distinguished into form, waviness and roughness (DigitalSurf 2013)

The following four components can be distinguished within 3D surface data: form, waviness, roughness and micro-roughness. Surface texture data is the information about the surface which remains when the surface form data has been removed (or 'filtered'), thus leaving waviness and roughness (Seah and De Chiffre 2011). For further information about the effect of filtering on surface texture measurement the reader is referred to Appendix 1 'A glossary of general terms used in surface texture analysis.

Traditionally, the 2D roughness average (Ra) has been the most commonly quoted parameter used to express roughness (Leach 2010). Despite it being widely assumed that Ra is the most relevant

surface texture parameter for dental erosion research, solely quoting Ra values in dental erosion research has many limitations which may adversely affect the usefulness of surface texture measurement for dental erosion (Nowicki 1985; Field, Waterhouse et al. 2010; Leach 2010). For example, the traditional Ra value contains no information about the 3D textural characteristics of a profile and limited information about factors such as the likelihood of future wear or wear-resistance, the potential rate of future wear or the potential of the enamel surface to retain fluids or surface treatments such as oral care products developed to counter the effects of dental erosion, including toothpastes, mouth rinses and varnishes. Moreover, the Ra value does not take into account the uniquely exquisite structure of human enamel, such as the prismatic nature of the tissue which may be affected by pre- or post-eruptive hard tissue defects and pathologies.

Surface texture measurement of dental erosion using modern 3D areal surface texture parameters has therefore greater potential relevance than 2D roughness parameters which are solely derived from single line profiles (International Organisation of Standardization 2010). This is because knowledge about the pathophysiology of erosive lesions, which as illustrated in Figure 1 above, in the early lesion involves subtle microscopic optical and mechanical surface changes (without bulk loss of tissue) to later macroscopic surface changes with irreversible loss of bulk tissue can be used to characterise the entire surface under investigation.

3D parameters are written with the capital letter S followed by a suffix of one or two small letters and provide the full characterisation of the 3D (areal) surface texture (Leach 2010). They are calculated using the entire surface, in contrast 2D parameters, which are calculated by averaging estimations using a number of single line profiles.

Table 4 and Table 5 below show the parameter abbreviations with their descriptions that are of interest in this study.

Table 4 Height 3D surface texture parameters (International Organisation of Standardization 2010)

Parameter	Description
Sa	Arithmetical mean height of the surface
Sq	Root mean square height of the surface
Ssk	Skewness of height distribution
Sku	Kurtosis of height distribution
Sp	Maximum height of peaks
Sv	Maximum height of valleys
Sz	Maximum height of the surface

Table 5 Functional 3D surface texture parameters (International Organisation of Standardization 2010)

Parameter	Description
Smr	Surface bearing area ratio (c = 0 nm under the mean plane)
Smc	Height of surface bearing area ratio (p = 10%)
Sxp	Peak extreme height (p = 50% q = 97.5%)

For further description of these parameters, the reader is referred to Appendix 1 ‘A glossary of general terms used in surface texture analysis’ on page 61 below.

Aims of the study

The overall aim was to investigate the effect of acid-mediated erosive enamel wear on the micro-texture of polished and non–polished human enamel *in vitro*.

The objectives were to determine which parameter or set of parameters, based on 3D measurement of surface texture, can be used to characterise the effect of enamel demineralisation by acid erosion and enamel remineralisation by human saliva, with reference to established methods for measuring tooth wear (surface microhardness and non-contacting profilometry), in early enamel erosion lesions on both polished and natural enamel surfaces *in vitro*.

The null hypothesis is that surface texture analysis with a 3D confocal laser scanning microscope used in combination with ISO 25178 surface texture analysis software will not be able to characterise the development of early *in vitro* erosive lesions and their remineralisation by human saliva in polished and unpolished human enamel *in vitro*.

Materials and Methods

2.1 Sample preparation

20 human third molars were collected from patients who required extraction of their third molar and who consented to using their teeth for this research project (Ethics Committee Approval reference 09/H0808/109). Enamel sections were firstly prepared using a water-cooled diamond wafering blade (XL 12205, Benetec Ltd., London, UK) to section the crown from the roots, following which the crown was further sectioned mesio-distally to provide two enamel sections per tooth. Each enamel section was then placed enamel side outwards in a sample forming device (Syndicad Ingenieurbüro, München, Germany) and samples were embedded in a self-curing bis-acryl composite (Protemp™4, 3M ESPE, Seefeld, Germany) to result in a 5 mm x 2.5 mm x 2 mm composite sample with an enamel section in the centre with the buccal or lingual surface facing upwards.

Figure 5 Photograph of the sample forming device used to embed the enamel sections in bis-acryl composite

This resulted in 40 human enamel samples, which were then randomly distributed into 2 groups (n=20/gp). Group 1 samples were polished flat and Group 2 samples were unpolished, thus mimicking the natural enamel surface, as shown in Figure 6 below.

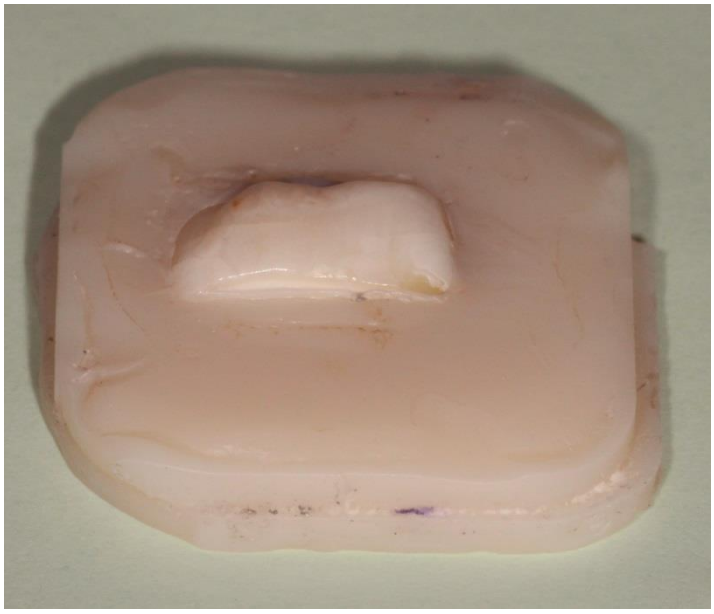

Figure 6 Photograph of unpolished enamel sample

The samples allocated to the polishing process were subjected to a grinding-polishing protocol in order to remove the outer enamel thus creating a flat enamel surface with uniform surface texture. The samples were polished in water-cooled rotating polishing machine (Meta-Serv 3000 Grinder-Polisher, Buehler, Lake Bluff, Illinois, USA) with a semi-automated polishing head (Vector LC Power Head, Buehler, Lake Bluff, Illinois, USA) under copious water irrigation and sequential use of 500, 1200, 2400 and 5000 grit silica carbide discs (Versocit, Struers A/S, Copenhagen, Denmark). As shown in Figure 7 below, this resulted in an exposed area of enamel, which was around 5 mm x 3 mm in area with a flatness tolerance of 0.4 μm and uniformly minimal surface textural features.

Figure 7 Photograph of polished enamel sample

In order to create references areas, PVC tape was placed laterally over the enamel to protect the lateral 1.5 mm of enamel, thus leaving a central 1.5 mm x 3 mm area of the enamel surface exposed to the *in vitro* erosive protocol.

2.2 Cyclic erosion model

All group 1 and group 2 samples were then subjected to an *in vitro* erosion model utilising a citric acid solution for enamel erosion and pooled human saliva for remineralisation in order to simulate an early enamel erosion lesion *in vitro*, as described by Young and Tenuata (2011).

A 0.3 % citric acid solution was prepared by adding citric acid power (Sigma-Aldrich, Poole, Dorset, UK) to distilled water, following which the pH was adjusted to 3.2 using a sodium hydroxide buffer and a calibrated pH meter and electrode (Oakton pH 510 Benchtop Meter with a WD-35801-00 pH electrode, (Eutech Instruments, Nijkerk, Netherlands). The solution had a titratable acidity of 19.5 ml, measured as the volume of 0.1 M solution of sodium hydroxide required to raise 20 millilitres of citric acid solution to pH 7.0 by adding increasing volumes of sodium hydroxide solution followed by agitation and equilibrium for two minutes until the pH reached 7.0.

Each sample was immersed in 50 ml of the citric acid solution at room temperature for the following time points: 30 seconds, 1 minute, 2 minutes and 5 minutes, after which the samples were rinsed in distilled water and allowed to dry before measurement. The tape was also removed for measurement of the eroded enamel surface and then repositioned after measurement.

Following erosion, the samples were rinsed in distilled water and then immersed in pooled human saliva to allow remineralisation of the eroded enamel lesions. The pH of the saliva was 7.1 and the calcium content was 1.4 mmol/l. Each sample was immersed in the 20 ml of the saliva at room temperature for the following time intervals 1 hour, 6 hours, 12 hours and 24 hours. After each rinsing period the samples were removed from the saliva, rinsed in distilled water and allowed to dry before measurement, with the tape being removed and replaced as during the erosion.

2.3 Measurement techniques

All polished samples (Group 1) were measured using Knoop microhardness, white light confocal profilometry and confocal laser scanning microscopy prior to the erosion / remineralisation. Subsequently, the polished samples were re-measured after 30 seconds, 1 minute, 2 minutes and 5 minutes of erosion and after 1 hour, 6 hours, 12 hours and 24 hours of remineralisation.

For the unpolished samples (Group 2), only the surface texture of the enamel surface was measured using confocal laser scanning microscopy, both prior to the erosion / remineralisation and subsequently at the four erosion and remineralisation time points. This was because of the inability to be able to measure the diamond indents in the curved enamel and also due to the lack of flattened reference areas for measurement of step height enamel loss.

2.3.1 Knoop Microhardness

A Knoop Microhardness Tester (Duramin-5, Struers Ltd, Rotherham, UK) was used to measure Knoop microhardness in this study, in order to quantify the effect of the citric acid erosion and human saliva remineralisation on the mechanical properties of the enamel surface. Figure 8 below shows the microhardness measurement protocol, which involved making 3 indentations in the centre of the erosion lesion, with each indentation having 100 µm spacing between indents. The accuracy of the tester had been previously investigated (Austin 2011) and was found to be 39.33 KHN.

3 indentations with
Knoop diamond
200 grams force
5 sec dwell time
100 microns spacing

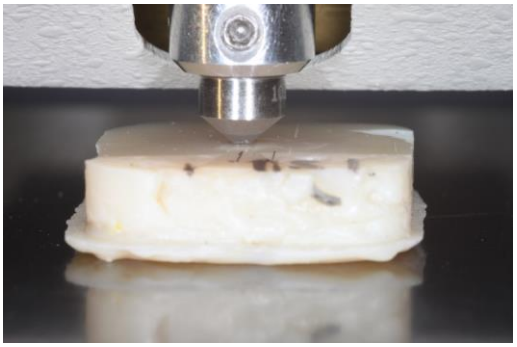

Image capture
X 40 lens

Measurement of indentation length (µm)
Conversion to Knoop Hardness using ASTM formula
HK = Constant x test force / indent diagonal squared

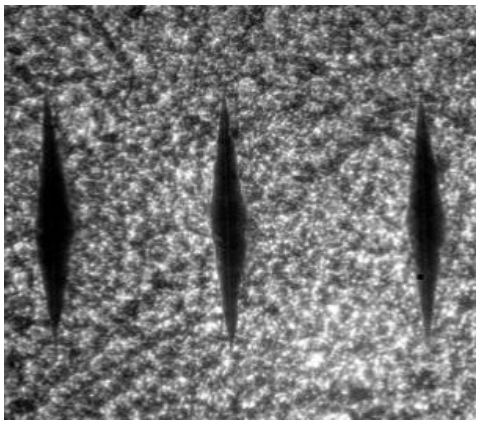

Figure 8 Measurement protocol for Knoop microhardness testing of enamel erosion and remineralisation

Samples were placed on the stage and the centre of the erosion lesion was brought into focus using the x40 objective lens. The area to be indented was selected and confirmed as being crack and defect free, with relatively flat and uniform surface morphology. If the form of the surface was too curved then a uniform indent was not possible and a close adjacent area was chosen instead.

Having selected the area, each indent was made using a Knoop diamond indenter which had longitudinal edge angles of 172.30° and 130°. The diamond indenter was loaded with 200 grams

force throughout a dwell time of 5 seconds per indent. For the image capture the x 40 lens was used to focus on the indents on the eroded enamel surface and an image was captured for later measurement as a .jpeg file.

Subsequent measurement of the indentation length was carried out using the Duramin measurement software. The length of each indentation was measured in μm and the Knoop hardness number (KHN) of the indentations was calculated according to the American Society for the Testing of Materials (ASTM) formula for calculation of the Knoop Hardness Number (KHN), as shown in Equation 1 below.

Equation 1 The American Society for the Testing of Materials (ASTM) formula for calculation of the Knoop Hardness Number (KHN)

$$KHN = \frac{F}{C_P \, L^2}$$

Where F is the load (kg) and L is the length of the long diagonal (mm). C_P is the indenter constant which, as shown in Equation 2 below, is 0.07028 for an indenter with ideal geometry (α angle of 172.5° and β angle of 130° between the opposite edges of the vertex of the diamond).

Equation 2 Indenter constant defined by the angulation of the opposite edges of the vertex of the Knoop diamond indenter

$$C_P = \frac{\tan(\beta/2)}{2\tan(\alpha/2)}$$

2.3.2 White-light confocal profilometry

A white-light confocal profilometer (XYRIS™ 4000 WL TaiCaan Technologies Ltd., Southampton, UK) was used to measure the enamel surface topography during the erosion/ remineralisation stages in order to confirm that the erosion model was simulating an early enamel lesion without bulk loss of enamel. A 5 mm x 3 mm scan area was imaged with a 10 µm step-over distance (in the x and y axes) in medium precision measurement mode, which generated a surface topography map of 301 y-axis profiles. For step height analysis of enamel surface changes, the resulting images were analysed using MountainsMap® surface analysis software (MountainsMap® v. 6.2; SARL Digital Surf, 16 rue Lavoisier, 25000 Besançon, France). The depth of the area of eroded enamel in relation to the area of sound reference enamel was calculated following ISO 5436-1 (2000) for step height measurement, whereby the central 1/3 of the width of the eroded enamel was used to analyse the average depth of the step, calculated from the datum plane.

The measurement uncertainty of the this measurement protocol had previously been determined (Austin 2011) following metrological good-practice guidelines (Bell 2010) which resulted in a standard combined uncertainty of measurement of step height of enamel loss of 0.28 µm.

2.3.3 Confocal Laser Scanning Microscopy

For both polished and unpolished samples, a 3D confocal laser scanning microscope (LEXT OLS4100, Olympus, Tokyo, Japan) was used to measure the surface texture of the enamel surface during the erosion and remineralisation. The instrument was housed in the Dimensional Nanometrology division of the National Physical Laboratory (National Physical Laboratory, Teddington, UK; http://www.npl.co.uk/science-technology/dimensional/dimensional-nanometrology/surface-topography-measurement) and is therefore a calibrated industry standard instrument for quantitative 3D surface texture measurement, with traceability to national measurement standards.

Figure 9 LEXT OLS4100 confocal laser scanning microscope (Olympus, Tokyo, Japan) used to measure surface texture of enamel samples

For each enamel sample 5 measurements across the entire surface area were made using the 50x objective lens with a 129 µm x 129 µm field of view and an NA of 0.95. The Z pitch setting was set to "fine" and the diameter of the laser beam used was 0.2 µm with 405 nm wavelength. The resolutions used in the X, Y, and Z axes were 0.02 µm, 0.02 µm, and 0.01 µm, respectively.

Calibration standards were used on the X, Y and Z axes of the 50x lens. These calibration standards have traceability to the National Institute of Advanced Industrial Science and Technology (AIST) of the National Metrology Institute of Japan. For the X and Y axes calibration of a 5 µm step height standard (OLS4KC01, LEXT OLS4100, Olympus, Tokyo, Japan) was used. For the Z axis calibration a 1.040 µm Skp standard was used (OLS4KC02, LEXT OLS4100, Olympus, Tokyo, Japan). All measurements were made at 21°C ±0.1°. The results of this calibration exercise revealed that the accuracy of the magnification in the X and Y axes was ±1.38 % and ±0.85 % respectively and the accuracy of the measurement difference in the Z direction was 0.013 µm.

Following calibration, initial scanning was carried out of a previously eroded enamel sample in order to determine the optimal image processing workflow. Images were imported into MountainsMap® for analysis and a workflow was determined following pilot work and discussion with Dimensional Nanometrology scientists at the National Physical Laboratory.

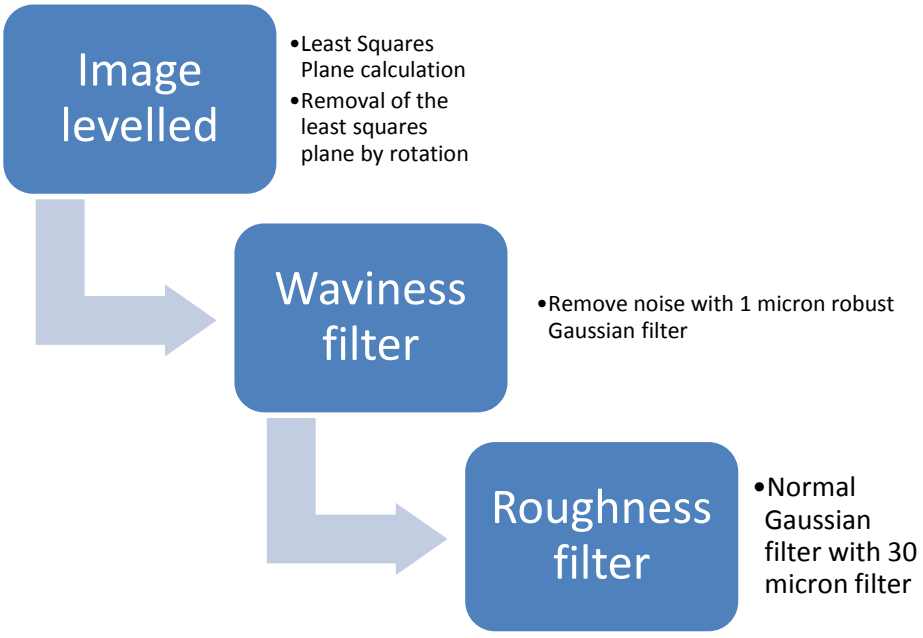

Figure 10 Overall image analysis workflow using MountainsMap® surface texture analysis software

Images were firstly levelled by removing the Least Squares plane from the surface to level the surface. Following the levelling of the surface, two levels of filtering were carried out in order to

highlight the relevant features of interest, which for the purposes of the present study, were the etching patterns of dental enamel created by the application of an acid to the enamel surface (Berkovitz 2009). This can be seen from the 3D surface texture image of an eroded enamel surface shown Figure 11 below.

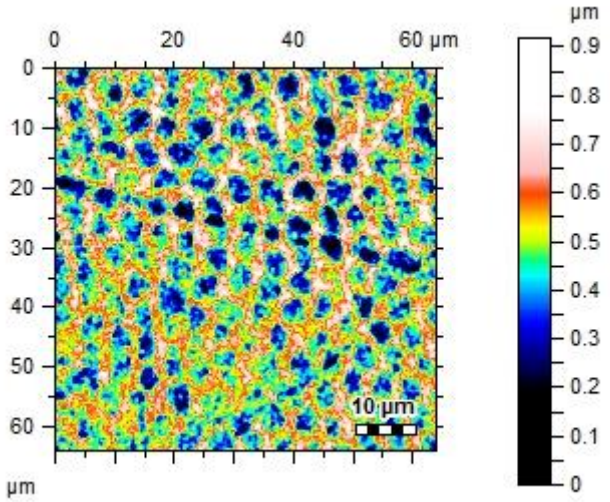

Figure 11 3D surface texture image of eroded enamel using a confocal laser scanning microscope (Olympus LEXT 4000)

In order to determine the optimal filtering sequence, using the Grains and Particles module in MountainsMap® surface texture analysis software, these enamel prisms were identified and their mean diameter was measured, which as shown in Figure 12 below was approximately 6 µm across. Therefore, for the purposes of this present study this was considered the size of feature of interest, in order to inform the selection of the appropriate filters.

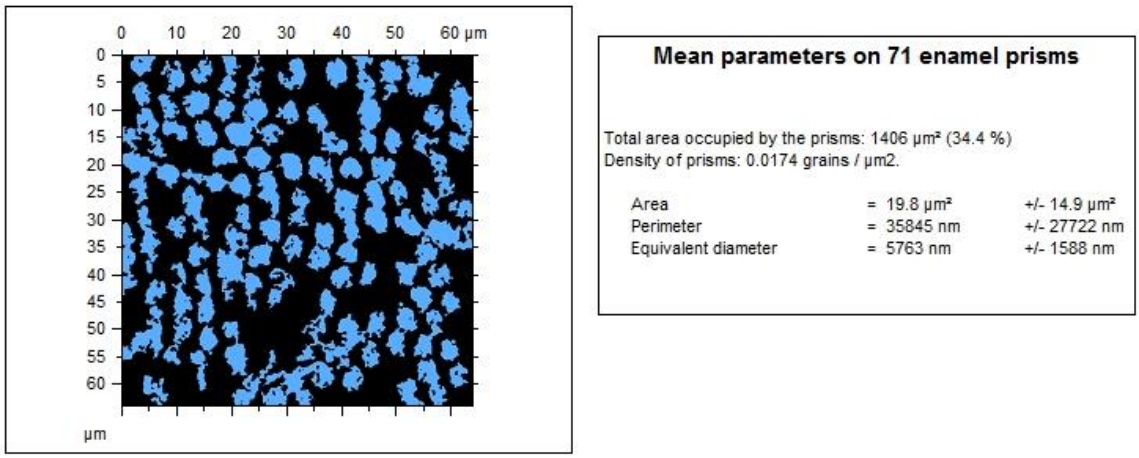

Figure 12 Exported image and parameter table of an eroded enamel surface showing the identification of enamel prism pattern characteristics for measurement of the mean prism diameter using MountainsMap® surface analysis software

Taking this into account, two levels of filters were applied. Firstly, a low-pass waviness filter, approximately 1/5th of the wavelength of the feature of interest (i.e. the diameter of an enamel prism), using a 1 µm robust Gaussian filter to the enamel surface. The effect of this primary filter can be seen in Figure 13 below.

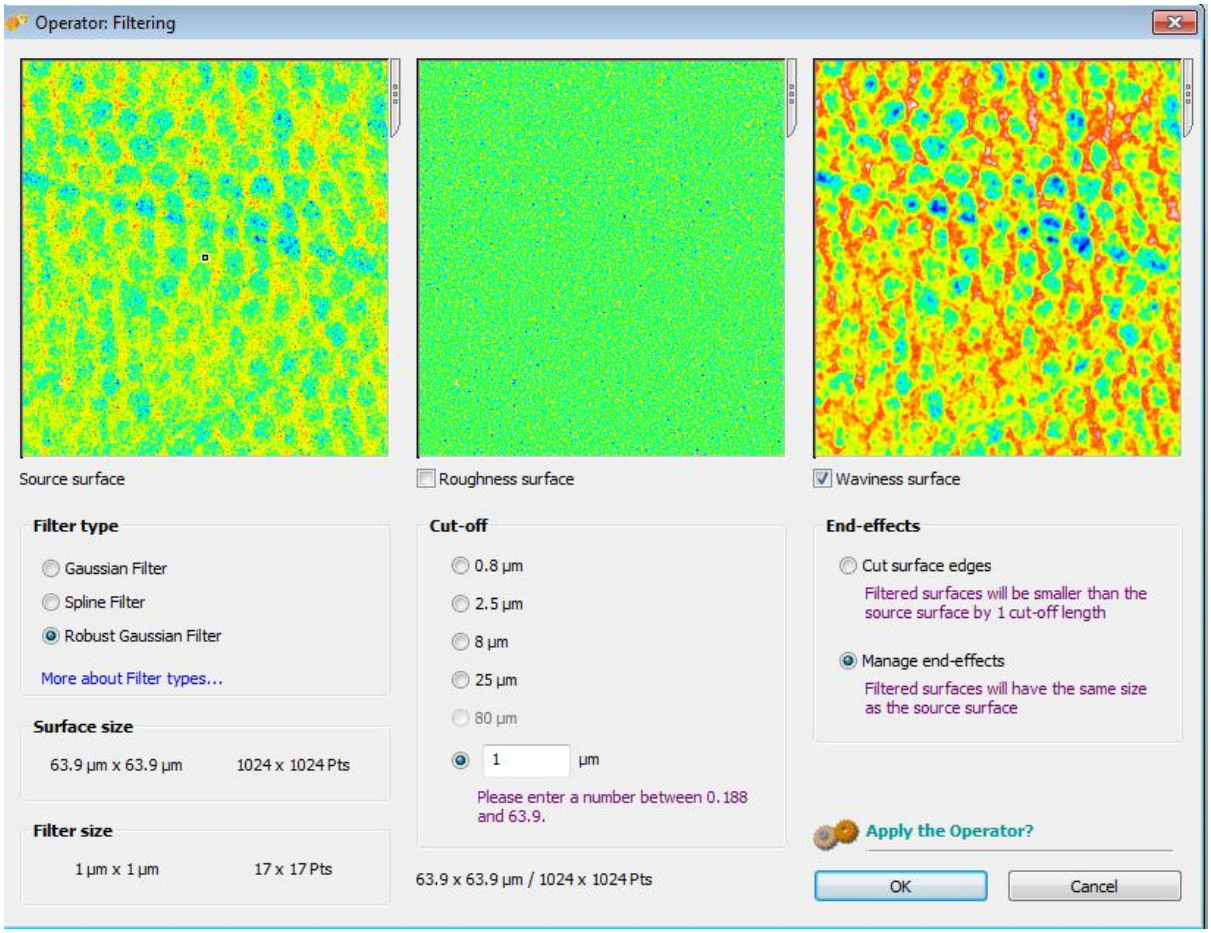

Figure 13 Effect of the initial low-pass 1 µm robust Gaussian waviness filter on the eroded enamel surface

Following this, a secondary high-pass 30 µm Gaussian roughness filter was applied to the resulting waviness output. This was chosen to be approximately 5 times the wavelength of the feature of interest (i.e. the 6 µm diameter prismatic structure), which would therefore isolate the features on the eroded enamel surface and allow the relevant 3D surface texture parameters to characterise the surface as comprehensively as possible. The effect of this secondary filter can be seen in Figure 14 below.

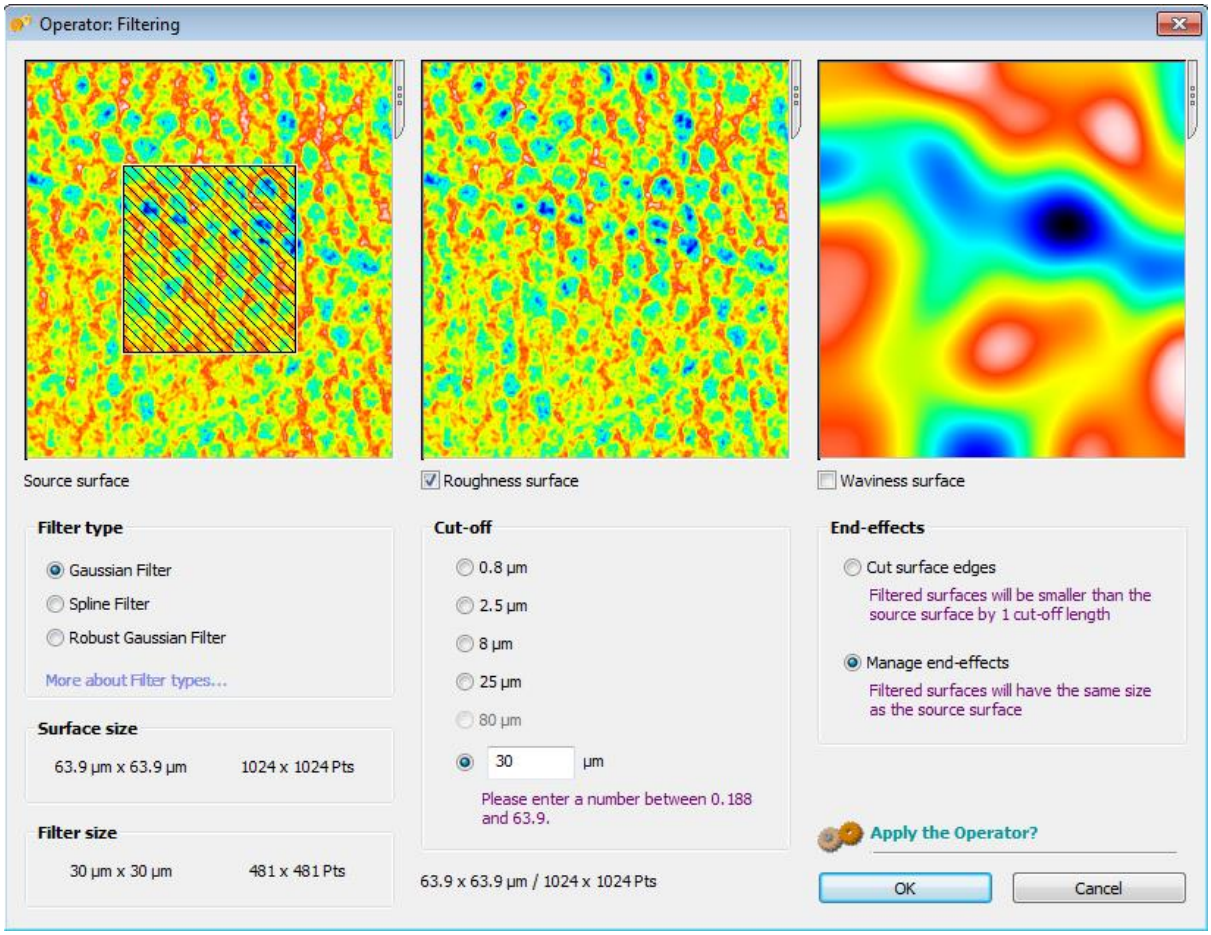

Figure 14 Effect of the secondary high-pass 30 µm Gaussian roughness filter on the eroded enamel surface

Once this protocol had been developed, ten 3D areal surface texture parameters of the worn enamel surfaces were calculated following ISO 25178 (International Organisation of Standardization 2010). The first seven parameters related to the height characteristics of the enamel surface, which, as seen in Table 6 and Appendix 1 below, involve calculations based on the statistical distribution of height values along the z axis. The remaining three parameters related to the functional characteristics of the enamel surface, which as can be seen in Table 7 below and Appendix 1 below, are the parameters commonly used in tribological studies of engineering surfaces and involve calculations from the material ratio curve (Abbott-Firestone curve).

Table 6 Height parameters calculated from the statistical distribution of height values along the z axis (International Organisation of Standardization 2010)

Parameter	Description
Sa	Arithmetical mean height of the surface
Sq	Root mean square height of the surface
Ssk	Skewness of height distribution
Sku	Kurtosis of height distribution
Sp	Maximum height of peaks
Sv	Maximum height of valleys
Sz	Maximum height of the surface

Table 7 Functional parameters calculated from the material ratio curve (Abbott-Firestone curve) (International Organisation of Standardization 2010)

Parameter	Description
Smr	Surface bearing area ratio (c = 0 nm under the mean plane)
Smc	Height of surface bearing area ratio (p = 10%)
Sxp	Peak extreme height (p = 50% q = 97.5%)

2.4 Statistical analysis

Data were exported to an Excel spread sheet (Microsoft® Office Excel® 2010, Microsoft® Corporation, USA) and statistical analyses were performed using GraphPad Prism statistical software (GraphPad Prism version 6.00 for Windows, GraphPad Software, La Jolla California USA, www.graphpad.com) using the GraphPad Statistics Guide to guide the choice of analysis (GraphPad Software 2013)

Data were initially tested for normality using the D'Agostino-Pearson omnibus test (D'Agostino 1986). Most of the data conformed to a normal distribution and therefore means and standard deviations of the groups were reported.

For the characterisation of the erosion lesions, the 3D surface texture, step height enamel loss and surface microhardness data for the four erosion time points (i.e. 30 seconds, 1 minute, 2 minutes and 5 minutes) were compared with baseline values of the sound enamel using repeated measures one-way ANOVA, with the Greenhouse-Geisser correction. Tukey's multiple comparisons test was subsequently applied, with individual variances computed for each comparison and $P<0.05$ considered statistically significant.

For the characterisation of the remineralisation of the erosion lesions, the 3D surface texture, step height enamel loss and surface microhardness data for the four remineralisation time points (i.e. 1 hour, 6 hours, 12 hours and 24 hours) were compared with the erosion values of the eroded enamel surface at the maximal erosion time point (i.e. after 5 minutes of erosion) using repeated measures one-way ANOVA, with the Greenhouse-Geisser correction. Tukey's multiple comparisons test was subsequently applied, with individual variances computed for each comparison and $P<0.05$ considered statistically significant.

Following conventional use, the levels of statistical significance were illustrated graphically by the abbreviation (ns) and the use of star symbols (*). Non-statistically significant differences were

indicated by (ns). The number of stars indicated a statistically significant difference of varying levels: one star (*) indicated $P<0.05$, two stars (**) indicated $P<0.01$; three stars (***) indicated $P<0.005$ and four stars (****) indicated $P<0.001$. These star symbols were used on figures and tables throughout the results section to indicate the outcomes of the statistical analyses comparing the erosion values vs. baseline and the remineralisation values vs. 5 minutes erosion.

Results

3.1 Polished Enamel Samples (Group 1)

3.1.1 Knoop Microhardness

As shown in Figure 15 below, the mean (SD) Knoop microhardness of the polished enamel samples at baseline (before erosion or remineralisation) was 363 (11) KHN. After erosion in citric acid, there were statistically significant decreases in the microhardness at all the erosion time points in comparison to baseline (P<0.001). Each subsequent erosion time point resulted in further statistically significant reductions in the enamel microhardness, such that after 5 minutes of erosion the lowest mean (SD) microhardness value of 266 (10) KHN was reached (P<0.001 vs. baseline).

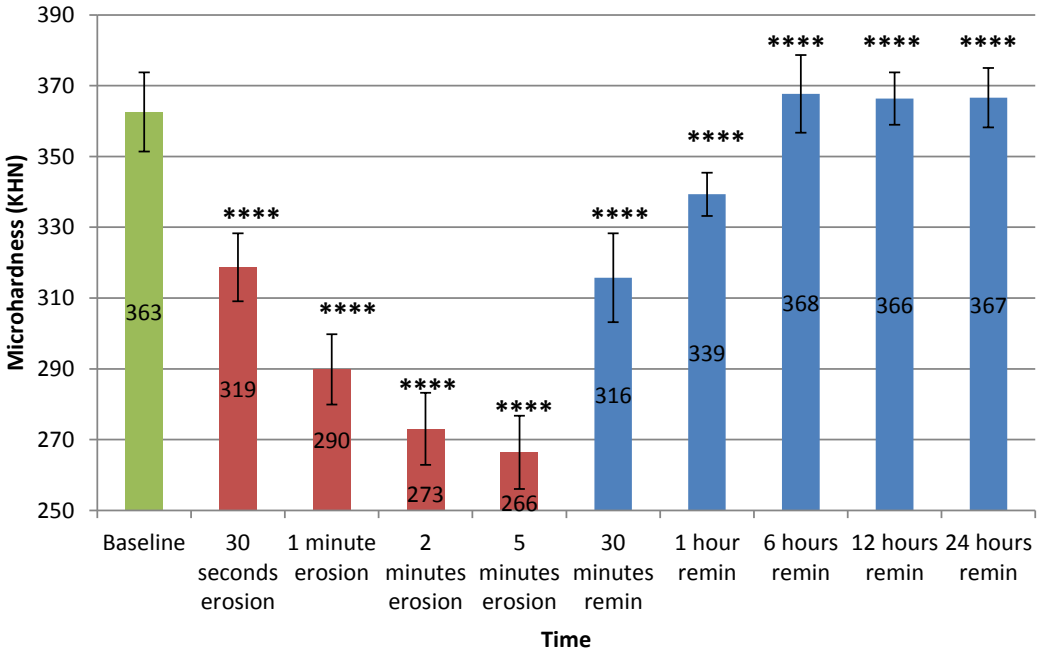

Figure 15 Mean (SD) enamel surface microhardness (KHN) at baseline (green bar); after citric acid erosion (red bars with statistical comparisons vs. baseline) and after remineralisation in pooled human saliva (blue bars with statistical comparison vs. 5 minutes erosion)

Subsequent immersion of the eroded samples in pooled human saliva resulted in a statistically significant increase in the surface microhardness at all the remineralisation times (P<0.001 vs.

erosion), with the microhardness of the enamel surface demonstrating sequential recovery in hardness over immersion times from a mean (SD) microhardness of 316 (13) KHN after 30 minutes remineralisation ($p<0.001$ vs. 5 minutes erosion). The enamel surface showed full recovery to the initial microhardness levels at baseline after 6 hours remineralisation 368 (11) KHN ($p<0.001$ vs. 5 minutes erosion).

3.1.2 White-light confocal profilometry

As shown in Figure 16 below, at baseline the enamel samples demonstrated no enamel step height loss. Although over the course of the erosion the mean (SH) enamel loss was seen to reach a maximum) step height of 0.46 (0.7) µm this was not statistically significant vs. baseline ($P>0.05$). This measured step height enamel loss appeared to reduce during the subsequent remineralisation in artificial saliva to reach a final mean (SD) step height enamel loss of 0.18 (0.55). However, this did not reach statistical significance in comparison either to baseline ($P>0.05$) or the enamel loss at 5 minutes of erosion ($p>0.05$).

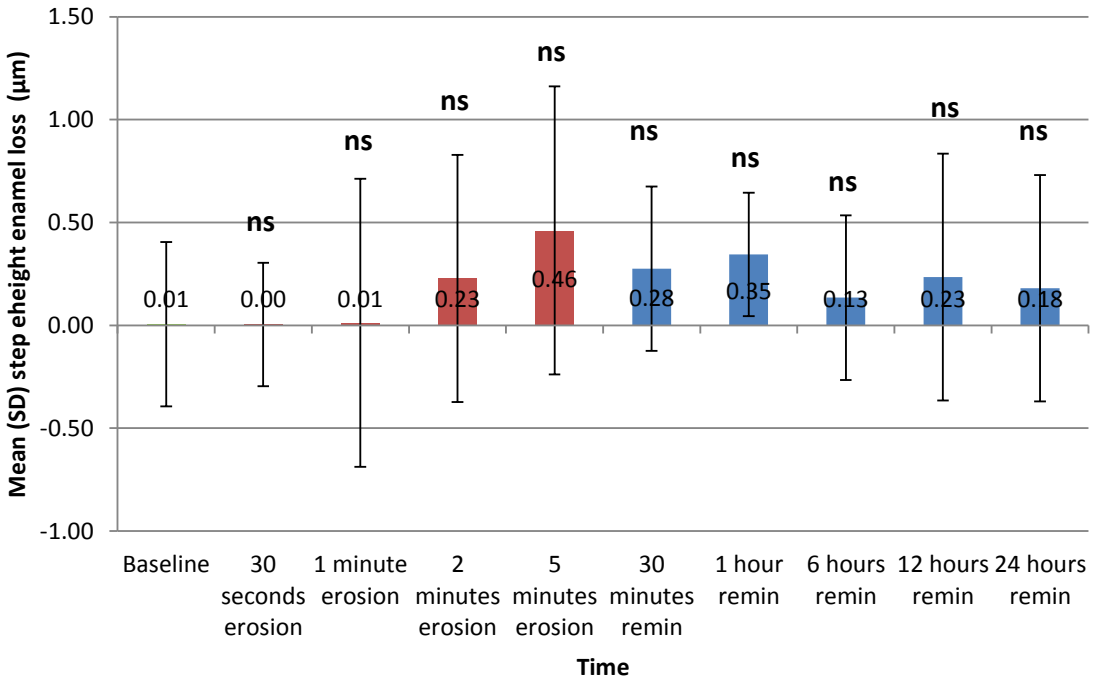

Figure 16 Mean (SD) step height enamel loss of the eroded enamel surface (µm) at baseline (green bar); after citric acid erosion (red bars with statistical comparisons vs. baseline) and after remineralisation in pooled human saliva (blue bars with statistical comparison vs. 5 minutes erosion)

3.1.3 Confocal Laser Scanning Microscopy

Figure 17 and Figure 18 below show example pseudo colour images and surface texture parameter outputs from MountainsMap® surface texture analysis software for an enamel sample at baseline and after 5 minutes of erosion respectively.

The pseudo-colour image at baseline (Figure 17) illustrates the very finest surface texture details that can be seen after polishing.

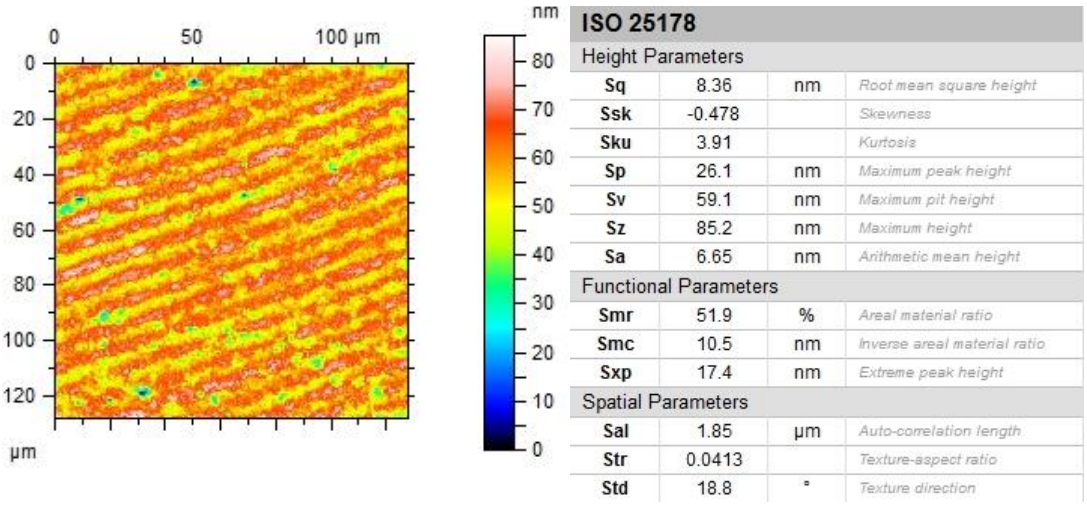

ISO 25178			
Height Parameters			
Sq	8.36	nm	*Root mean square height*
Ssk	-0.478		*Skewness*
Sku	3.91		*Kurtosis*
Sp	26.1	nm	*Maximum peak height*
Sv	59.1	nm	*Maximum pit height*
Sz	85.2	nm	*Maximum height*
Sa	6.65	nm	*Arithmetic mean height*
Functional Parameters			
Smr	51.9	%	*Areal material ratio*
Smc	10.5	nm	*Inverse areal material ratio*
Sxp	17.4	nm	*Extreme peak height*
Spatial Parameters			
Sal	1.85	µm	*Auto-correlation length*
Str	0.0413		*Texture-aspect ratio*
Std	18.8	°	*Texture direction*

Figure 17 Example of pseudo colour image and surface texture parameter output from MountainsMap® Surface texture analysis software for an enamel sample at baseline

This figure demonstrates a highly polished, flat and smooth surface with the presence of a feature of positive lines running parallel to each other, with a consistent spacing between the lines of between 8 µm to 10 µm, corresponding with incremental growth lines seen in enamel either from daily cross-striations or longer period striae of Retzius (Simmer, Papagerakis et al. 2010).

Figure 18 below illustrates an example pseudo colour image and surface texture parameter outputs from MountainsMap® for an enamel sample after 5 minutes erosion.

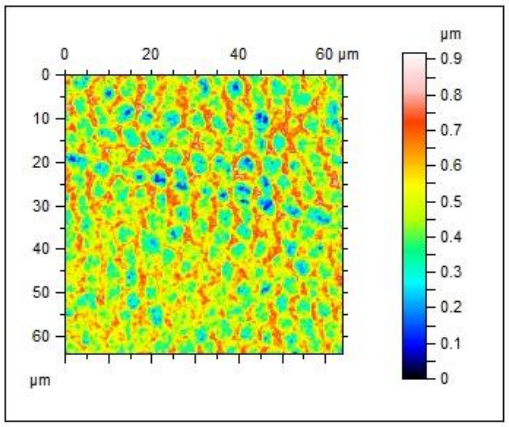

ISO 25178			
Height Parameters			
Sq	0.126	µm	*Root mean square height*
Ssk	-0.166		*Skewness*
Sku	2.78		*Kurtosis*
Sp	0.425	µm	*Maximum peak height*
Sv	0.494	µm	*Maximum pit height*
Sz	0.918	µm	*Maximum height*
Sa	0.102	µm	*Arithmetic mean height*
Spatial Parameters			
Sal	1.23	µm	*Auto-correlation length*
Str	0.585		*Texture-aspect ratio*
Std	94.2	°	*Texture direction*
Functional Parameters			
Smr	51.0	%	*Areal material ratio*
Smc	0.162	µm	*Inverse areal material ratio*
Sxp	0.258	µm	*Extreme peak height*

Figure 18 Example of pseudo colour image and surface texture parameter output from MountainsMap® Surface texture analysis software for an enamel sample after 5 minutes erosion

This sample demonstrates the typical pattern of eroded enamel showing the prismatic structure of enamel becoming clearly visible after 5 minutes of erosion in citric acid and the surface texture parameters correspondingly altering in comparison to the baseline sample image.

3.1.3.1 3D surface texture height parameters

Table 8 below shows the mean (SD) surface texture height parameters of the eroded enamel surface (µm) at baseline; after citric acid erosion (with statistical comparisons vs. baseline) and after remineralisation in pooled human saliva (statistical comparison vs. 5 minutes erosion).

Table 8 Mean (SD) surface texture height parameters of the eroded enamel surface (µm) at baseline; after citric acid erosion (with statistical comparisons vs. baseline) and after remineralisation in pooled human saliva (with statistical comparison vs. 5 minutes erosion)

	Baseline	Erosion in citric acid				Remineralisation in human saliva			
		30 seconds	**1 minute**	**2 minutes**	**5 minutes**	**1 hour**	**6 hours**	**12 hours**	**24 hours**
Mean (SD) Sa: Arithmetical mean height of the surface (µm)	0.008 (0.002)	0.02 (0.004) ***	0.05 (0.01) ****	0.07 (0.01) ****	0.09 (0.01) ****	0.09 (0.01) ns	0.06 (0.01) ****	0.03 (0.01) ****	0.03 (0.01) ****
Mean (SD) Sq: Root mean square height of the surface (µm)	0.011 (0.004)	0.02 (0.01) ns	0.06 (0.01) ****	0.09 (0.02) ****	0.11 (0.01) ****	0.14 (0.03) ****	0.08 (0.01) ****	0.04 (0.01) ****	0.04 (0.02) ****
Mean (SD) Ssk: Skewness of height distribution <no unit>	-1.25 (1.32)	-1.68 (0.75) ns	-0.94 (0.42) ns	-0.76 (1.04) ns	-0.20 (0.13) **	-0.22 (0.20) ns	-0.56 (0.73) ns	-0.52 (1.04) ns	-1.26 (0.76) **
Mean (SD) Sku: Kurtosis of height distribution <no unit>	13.30 (16.49)	9.97 (3.70) ns	6.37 (2.18) *	4.21 (1.76) ***	3.41 (0.32) ****	4.17 (1.09) ns	6.75 (3.41) ns	6.96 (3.06) ns	8.05 (4.34) ns
Sp: Maximum height of peaks (µm)	0.039 (0.016)	0.16 (0.17) ns	0.29 (0.10) **	0.42 (0.11) ****	0.56 (0.20) ****	0.76 (0.41) ns	0.47 (0.26) ns	0.39 (0.21) ns	0.26 (0.12) ***
Sv: Maximum height of valleys (µm)	0.134 (0.087)	0.27 (0.12) ns	0.83 (0.46) ****	0.75 (0.43) ****	0.69 (0.19) ****	0.82 (0.18) ns	0.58 (0.21) ns	0.47 (0.44) ns	0.41 (0.29) ns
Sz: Maximum height of the surface (µm)	0.174 (0.094)	0.42 (0.20) ****	1.27 (0.49) ****	1.17 (0.52) ****	1.25 (0.29) ****	1.52 (0.38) ns	1.05 (0.27) ns	0.86 (0.46) *	0.67 (0.39) ****

Analysis of the arithmetical mean height of the surface (Sa) revealed that at baseline the mean (SD) Sa was 8 (2) nm. These samples subsequently displayed statistically significant increases throughout the four erosion time points to reach a peak mean (SD) Sa of 0.09 (0.01) µm after 5 minutes immersion in citric acid ($P<0.001$). Initially, immersion of the eroded samples in pooled human saliva for 1 hour resulted in no statistically significant difference in the arithmetical mean height of the surface ($P>0.05$ vs. 5 minutes erosion). However, at all the subsequent remineralisation times there were sequential decreases in arithmetical mean height of the surface over immersion times to finally result in a mean (SD) Sa of 0.03 (0.01) µm. Although this value was statistically significantly reduced in comparison to 5 minutes of erosion ($P<0.001$) it still remained statistically significantly increased in comparison to baseline Sa values ($P<0.001$).

Analysis of the root mean square height (Sq) of the surface of the surface revealed that at baseline the mean (SD) Sq was 11 (4) nm. Initially, immersion of the eroded samples in citric acid for 5 minutes resulted in no statistically significant difference in the root mean square height of the surface ($P>0.05$ vs. baseline). However, these samples subsequently displayed statistically significant increases throughout the three erosion time points to reach a mean (SD) Sq of 0.11 (0.01) µm after 5 minutes immersion in citric acid ($P<0.001$). Subsequent immersion of the eroded samples in pooled human saliva for 1 hour resulted in a further statistically significant increase in the root square mean height of the surface ($P>0.001$ vs. 5 minutes erosion). However, after at all the subsequent remineralisation times there were sequential decreases in the root mean height of the surface over immersion times to finally result in a mean (SD) Sq of 0.04 (0.01) µm. Although this value was statistically significantly reduced in comparison to 5 minutes of erosion ($P<0.001$) it still remained statistically significantly increased in comparison to the baseline Sq values ($P<0.001$).

Analysis of the remaining surface texture height parameters (Ssk, Sku, Sp, Sv and Sz) revealed similar relationships between the values over the erosion time points. However over the remineralisation data showed that, unlike the other parameters, for the kurtosis of the height distribution (Sku) and the maximum height of the valleys (Sz) parameters there was not a statistically significant difference in the values after 24 hours of remineralisation in comparison to 5 minutes of erosion ($P>0.05$).

3.1.3.2 3D surface texture functional parameters

Table 9 below shows the mean (SD) surface texture functional parameters of the eroded enamel surface (μm) at baseline; after citric acid erosion (with statistical comparisons vs. baseline) and after remineralisation in pooled human saliva (statistical comparison vs. 5 minutes erosion).

Table 9 Mean (SD) surface texture functional parameters of the eroded enamel surface (µm) at baseline; after citric acid erosion (with statistical comparisons vs. baseline) and after remineralisation in pooled human saliva (with statistical comparison vs. 5 minutes erosion)

	Baseline	Erosion in citric acid				Remineralisation in human saliva			
		30 seconds	1 minute	2 minutes	5 minutes	1 hour	6 hours	12 hours	24 hours
Smr: Surface bearing area ratio below the mean plane (%)	53.47 (2.45)	58.07 (2.13) ****	53.83 (1.26) ns	52.28 (2.02) ns	51.15 (0.58) ***	50.98 (0.98) ns	53.65 (1.07) ***	54.65 (2.66) ****	57.65 (0.57) ****
Smc Inverse Areal Material Ratio p=10 % (µm)	0.012 (0.003)	0.02 (0.01) ns	0.08 (0.01) ****	0.11 (0.01) ****	0.14 (0.02) ****	0.14 (0.02) ns	0.09 (0.01) ****	0.05 (0.02) ****	0.03 (0.01) ****
Sxp Extreme Peak Height p= 50 % and q=97.5 % (µm)	0.023 (0.01)	0.06 (0.02) ***	0.14 (0.03) ****	0.19 (0.04) ****	0.23 (0.02) ****	0.25 (0.02) ns	0.17 (0.04) ****	0.09 (0.03) ****	0.08 (0.02) ****

Analysis of these surface texture functional parameters (Smr, Smc and Sxp) revealed similar relationships between the values over the erosion time points as for the surface texture height parameters. After 5 minutes of erosion all functional texture parameters demonstrated statistically significant differences in comparison to baseline ($P<0.005$). Equally, the remineralisation data showed that there was a statistically significant difference in the values after 24 hours of remineralisation in comparison to 5 minutes of erosion for all three functional parameters ($P<0.001$).

3.2 Unpolished Enamel Samples (Group 2)

3.2.1 Confocal Laser Scanning Microscopy

Figure 19 below shows a 3D image of a representative unpolished enamel sample at baseline prior to analysis with MountainsMap® surface texture analysis software. This image at baseline illustrates both the flatness deviation of the curved sample surface as well as the heterogeneity in the surface texture across the 129 µm x 129 µm area.

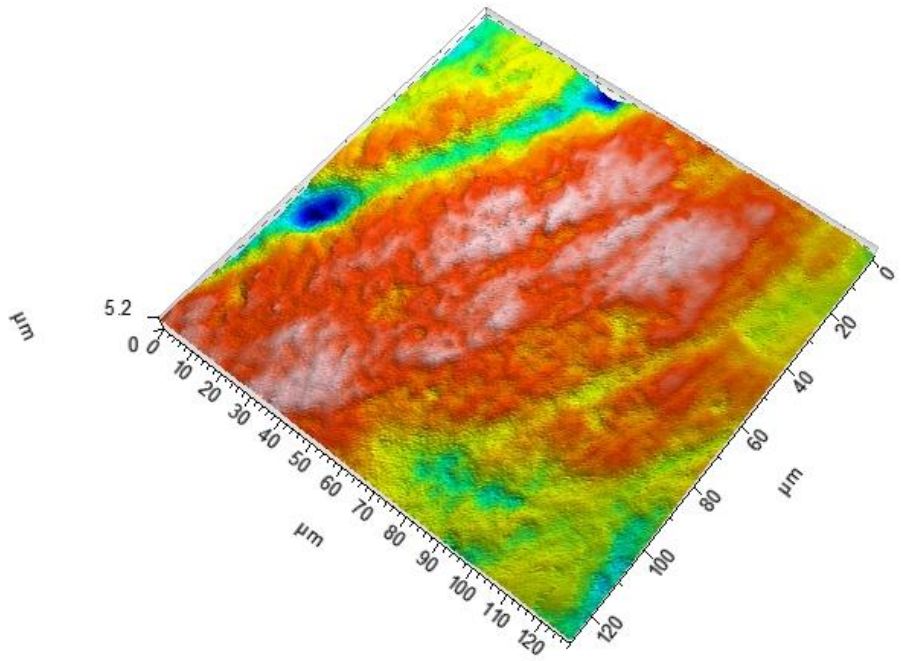

Figure 19 Example 3D image of a representative unpolished enamel sample at baseline prior to analysis with MountainsMap® surface texture analysis software

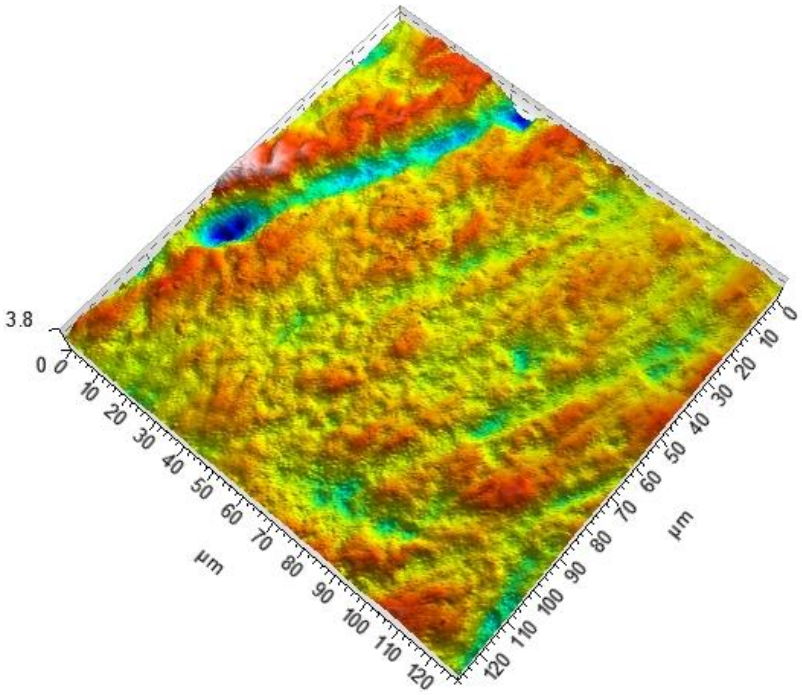

ISO 25178			
Height Parameters			
Sq	0.390	µm	*Root mean square height*
Ssk	-1.06		*Skewness*
Sku	5.91		*Kurtosis*
Sp	1.48	µm	*Maximum peak height*
Sv	2.33	µm	*Maximum pit height*
Sz	3.81	µm	*Maximum height*
Sa	0.285	µm	*Arithmetic mean height*
Functional Parameters			
Smr	55.9	%	*Areal material ratio*
Smc	0.429	µm	*Inverse areal material ratio*
Sxp	1.01	µm	*Extreme peak height*

Figure 20 Example 3D image of a representative unpolished enamel sample at baseline after analysis with MountainsMap® surface texture analysis software and the corresponding parameters output table

Figure 20 above shows an example 3D image of a representative unpolished enamel sample at baseline after analysis with MountainsMap® surface texture analysis software and the corresponding parameters output table. This figure demonstrates a highly rough surface with the presence of surface texture features including negative lines or scratches running across the surface, with what appears to be already exposed prismatic structures in the roughness.

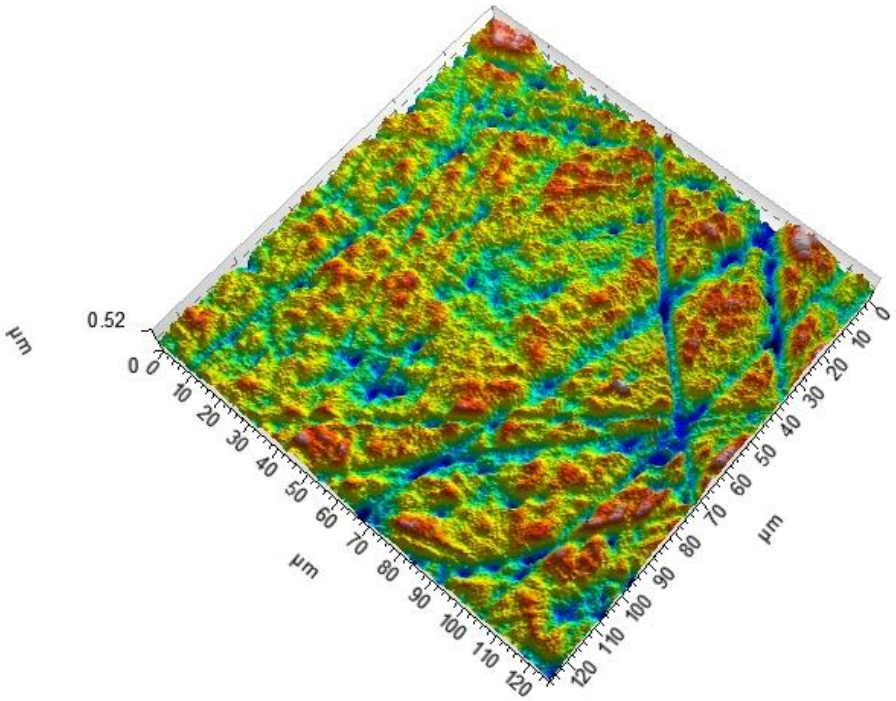

ISO 25178			
Height Parameters			
Sq	0.0795	µm	*Root mean square height*
Ssk	-0.359		*Skewness*
Sku	3.04		*Kurtosis*
Sp	0.248	µm	*Maximum peak height*
Sv	0.273	µm	*Maximum pit height*
Sz	0.521	µm	*Maximum height*
Sa	0.0632	µm	*Arithmetic mean height*
Functional Parameters			
Smr	53.3	%	*Areal material ratio*
Smc	0.0967	µm	*Inverse areal material ratio*
Sxp	0.181	µm	*Extreme peak height*

Figure 21 Example 3D image of a representative unpolished enamel sample after 5 minutes erosion with MountainsMap® surface texture analysis and the corresponding parameters output table

Figure 21 above shows a 3D image of a representative unpolished enamel sample after 5 minutes erosion with MountainsMap® surface texture analysis parameters output table. This figure also demonstrates a highly roughened surface with the presence of the negative lines or scratches running in an apparently random fashion across the enamel surface. The prismatic pattern of the eroded enamel structure is not readily apparent due to the extent of the variation in the surface topography and texture.

As can be seen in Table 10 (Mean (SD) surface texture height parameters of the eroded unpolished enamel surface (µm) at baseline; after citric acid erosion with statistical comparisons vs. baseline and after remineralisation in pooled human saliva with statistical comparison vs. 5 minutes erosion) and Table 11 (Mean (SD) surface texture functional parameters of the eroded unpolished enamel surface (µm) at baseline; after citric acid erosion with statistical comparisons vs. baseline and after remineralisation in pooled human saliva with statistical comparison vs. 5 minutes erosion) below, there were almost no statistically significant differences in the enamel surface texture after 5 minutes of erosion in comparison to baseline ($P>0.05$), neither were there any statistically significant differences in the enamel surface texture after 24 hours remineralisation in human saliva in comparison with 5 minutes erosion ($P>0.05$). There was a statistically significant decrease in the mean (SD) Sa: arithmetical mean height of the surface (µm) from 0.2 (0.1) µm at baseline to 0.12 (0.06) after 5 minutes of erosion ($P<0.05$) and this remained statistically significantly decreased in comparison to baseline Sa values after 24 hours remineralisation in human saliva ($P<0.001$).

Table 10 Mean (SD) surface texture height parameters of the eroded unpolished enamel surface (µm) at baseline; after citric acid erosion (with statistical comparisons vs. baseline) and after remineralisation in pooled human saliva (with statistical comparison vs. 5 minutes erosion)

	Baseline	Erosion in citric acid				Remineralisation in human saliva			
		30 seconds	**1 minute**	**2 minutes**	**5 minutes**	**1 hour**	**6 hours**	**12 hours**	**24 hours**
Mean (SD) Sa: Arithmetical mean height of the surface (µm)	0.20 (0.1)	0.19 (0.08) ns	0.14 (0.12) ns	0.14 (0.04) ns	0.12 (0.06) *	0.13 (0.06) ns	0.12 (0.06) ns	0.14 (0.06) ns	0.12 (0.06) ns
Mean (SD) Sq: Root mean square height of the surface (µm)	0.27 (0.14)	0.27 (0.15) ns	0.20 (0.17) ns	0.19 (0.06) ns	0.17 (0.07) ns	0.17 (0.07) ns	0.19 (0.04) ns	0.15 (0.07) ns	0.17 (0.07) ns
Mean (SD) Ssk: Skewness of height distribution <no unit>	-0.86 (0.61)	0.31 (1.8) ns	-0.14 (2.64) ns	-0.66 (1.45) ns	-1.19 (1.04) ns	-1.13 (1.05) ns	-1.20 (1.04) ns	-1.17 (0.05) ns	-1.18 (1.04) ns
Mean (SD) Sku: Kurtosis of height distribution <no unit>	4.85 (1.75)	13.71 (15.87) *	22.15 (35.62) ns	10.31 (11.23) ns	9.41 (9.31) ns	9.39 (9.35) ns	7.52 (9.15) ns	9.74 (6.31) ns	7.57 (9.31) ns
Sp: Maximum height of peaks (µm)	1.00 (0.69)	2.20 (1.77) *	1.53 (0.97) ns	1.14 (0.84) ns	1.01 (0.67) ns	1.25 (0.53) ns	1.02 (0.57) ns	1.08 (0.53) ns	1.06 (0.68) ns
Sv: Maximum height of valleys (µm)	1.59 (0.79)	1.72 (0.98) ns	1.55 (1.47) ns	1.46 (0.6) ns	1.40 (0.74) ns	1.75 (0.57) ns	1.57 (0.75) ns	1.28 (0.36) ns	1.84 (0.47) ns
Sz: Maximum height of the surface (µm)	2.59 (1.36)	3.92 (2.4) ns	3.08 (1.99) ns	2.60 (1.04) ns	2.41 (1.22) ns	2.26 (1.76) ns	2.79 (1.02) ns	2.76 (0.7) ns	2.98 (1.86) ns

Table 11 Mean (SD) surface texture functional parameters of the eroded unpolished enamel surface (µm) at baseline; after citric acid erosion (with statistical comparisons vs. baseline) and after remineralisation in pooled human saliva (with statistical comparison vs. 5 minutes erosion)

	Baseline	Erosion in citric acid				Remineralisation in human saliva			
		30 seconds	1 minute	2 minutes	5 minutes	1 hour	6 hours	12 hours	24 hours
Smr: Surface bearing area ratio below the mean plane (%)	54.90 (3.53)	37.64 (42.09) ns	34.03 (42.9) ns	60.38 (42.21) ns	61.90 (48.97) ns	67.56 (34.76) ns	60.58 (47.98) ns	60.59 (41.28) ns	65.79 (48.4) ns
Smc Inverse Areal Material Ratio p=10 % (µm)	0.28 (0.16)	0.28 (0.14) ns	0.20 (0.16) ns	0.20 (0.06) ns	0.18 (0.09) ns	0.17 (0.09) ns	0.18 (0.05) ns	0.17 (0.09) ns	0.18 (0.05) ns
Sxp Extreme Peak Height p= 50 % and q=97.5 % (µm)	0.59 (0.32)	0.58 (0.21) ns	0.48 (0.48) ns	0.47 (0.16) ns	0.40 (0.18) ns	0.46 (0.18) ns	0.33 (0.18) ns	0.36 (0.18) ns	0.43 (0.18) ns

Discussion

The results of this present study have demonstrated, for the first time (Lussi, Schlueter et al. 2011), that 3D surface texture analysis of polished enamel samples using confocal laser scanning microscopy is an effective analytical technique for quantitative characterisation of the minute surface changes that occur in human enamel during *in vitro* citric acid erosion ($P<0.001$ vs. baseline) and during *in vitro* human saliva remineralisation ($P<0.001$ vs. 5 mins erosion). The microhardness analysis demonstrated that the remineralisation in pooled human saliva resulted in a statistically significant recovery of the enamel microhardness at all the immersion times ($P<0.001$ vs. 5 minutes erosion). These sequential increases in microhardness over all the saliva immersion times corresponded with remineralisation re-hardening the surface, such that after 6 hours remineralisation, the enamel surface demonstrated mean (SD) surface microhardness values which were not statistically significant when compared to baseline ($P>0.05$). This was corroborated by the profilometry data which demonstrated that there was no significant enamel loss either after 5 minutes erosion ($P>0.05$), nor indeed after 24 hours remineralisation ($P>0.05$). The present *in vitro* model, therefore, simulated *in vitro* an early enamel erosion lesion with apparently reversible mechanical changes such that the enamel surface could be considered to have been completely remineralised from 6 hours immersion in saliva onwards (Young and Tenuta 2011).

However, in contrast to the established analytical techniques (Schlueter, Hara et al. 2011), the novel surface texture analyses of the remineralised enamel surface revealed statistically significant textural differences in comparison to polished enamel surface at baseline ($P<0.001$ vs. baseline). This therefore suggests that even initial erosion models cause pathological changes to the enamel surface which cannot be fully reversed (Young and Tenuta 2011). However, when the unpolished enamel samples were measured, the

surface texture analyses were not able to quantitatively characterise any erosion that was taking place. This may be a methodological limitation of the study, in that the filtering workflow was developed primarily with a flat enamel surface with a homogenous surface texture across the entire enamel surface, whereas the heterogeneity in the texture of the unpolished enamel surface would have affected the precision of repeated measurement, especially as the surface texture was calculated from five 129 µm x 129 µm scans of the enamel surface at each time point with the confocal laser scanning microscope.

However this finding of great baseline textural variability is also somewhat in agreement with recently presented data which required up to 150 minutes of exposure to orange juice for unpolished enamel samples to demonstrate changes in 2D roughness parameter which could be quantified with statistically significant differences (Jones, Chew et al. 2013). This finding of great variability in the baseline textural characteristics of unpolished enamel samples is also in agreement with a previous study which found that the surface texture of natural tooth surfaces varied widely depending on whether or not the tooth was erupted and in function (Las Casas, Bastos et al. 2008). Future investigations into erosion of curved enamel surfaces *in vitro*, *in situ*, or *in vivo* should therefore take into consideration the baseline surface textural characteristics. Nonetheless, the findings of the present study lend credibility to the possibility of using 3D surface texture analysis as a method for determining the aetiology of the specific wear processes the enamel surface has been subjected to. Previous engineering measurement research studies have successfully employed similar 3D surface texture analytical techniques to identify different wear processes occurring in deep drawing dies in the sheet metal industry which may present novel possibilities for dental erosion research (Christiansen and De Chiffre 1997).

The earliest method for assessment of surface texture was by simply running a fingernail across the surface of the object, a technique which led to the development of stylus

profilometers (Leach 2010). Subsequently, a wide variety of surface topography measurement instrumentation has been developed, with increasing sensitivity and ease of use. Contacting profilometers typically consist of a stylus that physically contacts the surface being measured and a transducer to convert its vertical movement into an electrical signal (International Organisation of Standardization 1996). One potential disadvantage of contacting profilometry is that the contacting stylus may damage the delicate demineralised surface layer of eroded enamel and thus the effect of the stylus force could have significant influence on the measurement results (Attin 2006; Schlueter, Hara et al. 2011). Moreover, as shown in Figure 22 below, contacting instruments have larger stylus diameter in comparison to non-contacting sensor diameters and therefore optical instruments can measure surface topography and roughness at a considerably higher resolution. For these reasons, non-contacting profilometry is usually preferred for dental erosion assessment of established wear lesions (Schlueter, Hara et al. 2011).

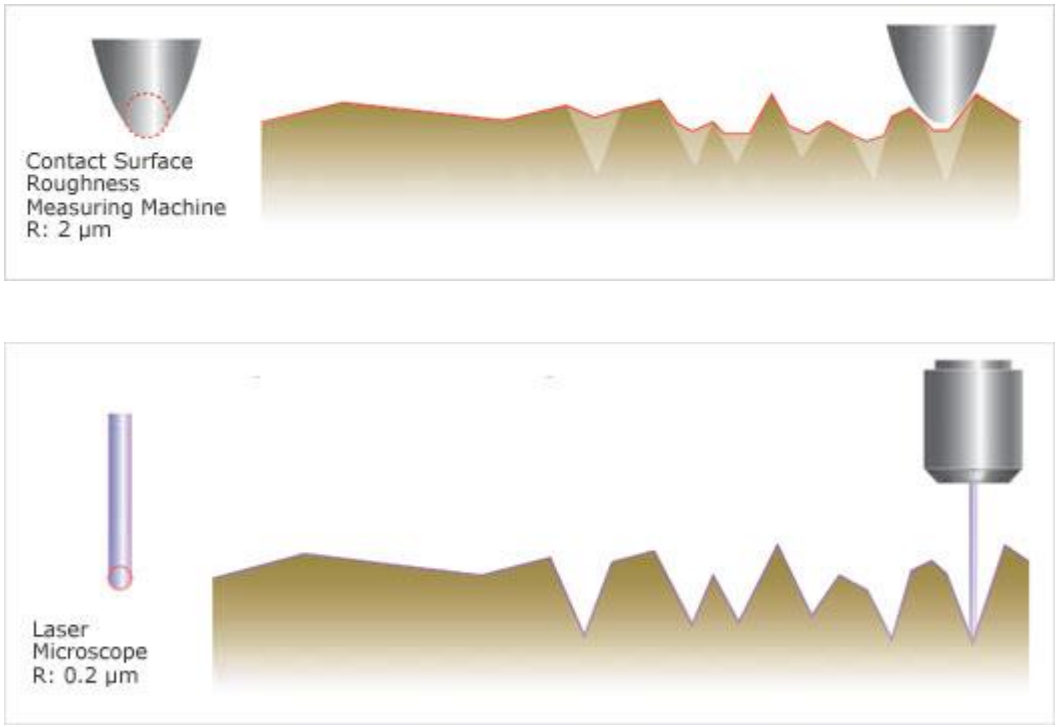

Figure 22 Illustration of the difference in surface measurement output between a contacting profilometer with a stylus radius of 2 µm and a non-contacting profilometer with a sensor radius of 0.2 µm.

Reflection mode confocal laser scanning microscopy relies on a laser light source (wavelength 405 nm for the Olympus LEXT 4000) to emit light which then passes through one pinhole and onto galvanometric mirrors which move a laser spot laterally across the sample surface, without physical table motion. The light reflected back from the focal plane passes through another pinhole before reaching a charge-coupled device sensor which results in one pixel being imaged at a time, with the result of many optical vertical sections having normal vectors aligned to the optical axis. These sections can then be reconstructed vertically to produce a topographic surface dataset.

Thus, confocal laser scanning microscopy provides more precise surface texture information than optical profilometry due to higher vertical resolution which can be in the range of nanometers, depending on the wavelength, numerical aperture and the smaller laser spot size, which translates into improved lateral resolution and therefore a more sensitive measurement of the surface texture (Field, Waterhouse et al. 2010; Seah and De Chiffre 2011). Until recently, confocal laser scanning microscopy was used in dental erosion research either to provide qualitative subsurface information using fluorescence or auto fluorescence (Duschner, Gotz et al. 2000; Schlueter, Hara et al. 2011) or in reflection mode to attempt to quantify bulk enamel loss using surface form measurement (Heurich, Beyer et al. 2010). However newer calibrated instruments have advanced the field of surface texture measurement for many purposes, both within the biological and engineering sciences (Leach 2010).

The calibration process employed prior to the start of this study was important to demonstrate that the instrument was ‘fit-for-purpose’ to use in this study (Bell 2010). The calibration revealed that for the X and Y axes the system was within the magnification error margin for the 50x objective lens which was required to be within ±2% of the calibration

result of the standard sample and for the Z axis this indicated that the measurement accuracy of 13 nm was within the requirements of the accuracy of this study.

Although there has recently been increased interest in the dental erosion research community into the use of advanced surface metrology analytical techniques to gain information about the surface texture of eroded enamel surfaces, these techniques have not, to date, been fully explored and exploited (Field, Waterhouse et al. 2010; Schlueter, Hara et al. 2011). These efforts are aimed both to further the understanding of the fundamental mechanisms underlying erosive tooth wear (Field, Waterhouse et al. 2010; Rakhmatullina, Bossen et al. 2011; Schlueter, Hara et al. 2011) and also to investigate the potential effectiveness of surface treatments in early erosion models *in vitro* (Zhang, Anderson et al. 2000; Jones, Chew et al. 2013). However, to date this is the first research study which has applied the latest 3D surface texture parameters to erosive wear of human enamel to characterise *in vitro* the height and functional features of the enamel surface as it is subjected to citric acid erosion and subsequent remineralisation in human saliva.

This current study has therefore highlighted that in polished enamel samples, 3D surface texture analysis is able elucidate information about the pre-eruptive developmental processes that result in the exquisitely hierarchical structure of enamel tissue morphology. The surface texture analysis of the polished enamel sample before erosion, as seen in the pseudo-colour image in Figure 17 above, illustrated the residual surface textural features that remain even after the finest polishing processes. These histological features were seen in Figure 17 as incremental lines running parallel to each other at a consistent spacing of between 8 µm to 10 µm. These appear to be the regularly occurring incremental markers that occur in enamel during the secretory stage of amelogenesis; either as daily cross-striations or long period striae of Retzius (SR lines). These lines correspond to what was the enamel surface at precise points in time during the secretory stage of amelogenesis, with

enamel being formed in humans at a rate of approximately 4 µm/ day for the daily cross striations (Risnes 1986) and the longer period striae of Retzius occurring at a periodicity of every 7-11 days (Reid and Ferrell 2006).

The surface texture analysis was also able to characterise the surface changes that occurred during early enamel erosion and remineralisation, results which were confirmed using microhardness. The 3D surface texture functional parameters provide information about how the enamel surface is likely to function in future when subjected to further mechanical and chemical pathological processes in its immediate oral environment which ultimately results in the clinical disease of erosive tooth wear. This may be useful in predicting which wear lesions will progress and which will not, a clinical challenge that remains challenging to quantitatively assess (Rodriguez, Austin et al. 2011). This present study therefore opens novel possibilities in enamel lesion characterisation and development for future investigations into erosive tooth wear with the ultimate aim of benefiting patients affected by tooth wear.

Conclusions

Referring back to the aims, it can be concluded that:

1. 3D height and functional surface texture parameters can be used to characterise the effect of enamel demineralisation by acid erosion and enamel remineralisation by human saliva, with reference to established methods for measuring tooth wear (surface microhardness and non-contacting profilometry), in early enamel erosion lesions in polished enamel surfaces *in vitro*.
2. The null hypothesis, which stated that quantitative 3D confocal laser scanning microscopy used in combination with ISO 25178 surface texture analyses, would not be able to characterise the development of early *in vitro* erosive lesions and their remineralisation by human saliva in polished human enamel has been rejected. However, for unpolished human enamel the null hypothesis has been accepted.

Future developments

1 Determine the optimal surface texture parameters for analysis of curved samples with a large degree of heterogeneity in surface texture and topography and determine a sample preparation process for curved enamel surfaces that mimics the oral environment.

2 Translate these *in vitro* results into *in situ* and *in vivo* studies investigating the potential effectiveness of surface treatments in early erosion models, such as toothpastes, mouth rinses and varnishes

3 Investigate the relationship between surface texture of eroded enamel samples and other non-destructive measurement techniques, such as optical coherence tomography, for investigating erosive wear of human enamel both *in vitro* and *in vivo.*

Appendices

Appendix 1 A glossary of general terms used in surface texture analysis (DigitalSurf 2013)

Abbott-Firestone Curve	Curve obtained by cumulating the values of the depths distribution, from the highest peak (0%) to the deepest valley (100%). The Abbott-Firestone curve allows you to calculate the bearing ratio that is useful for the functional characterisation of a sample.
Accuracy	The accuracy of a measurement system depends from the intrinsic factors of the instrument (particularly the resolution) and from environmental factors (vibrations, noise, etc.). The accuracy is the smallest value an instrument is able to measure with precision.
Amplitude parameters	Surface finish parameters class characterizing the distribution of heights. E.g. the Ra, Rq and Rz parameters are amplitude parameters.
Anisotropic / Anisotropy	A surface is said anisotropic when its characteristics are not identical in all directions of the measurement plane. These surfaces can, in general, not be characterised using profilometry, but require a 3-dimensional measurement of the relief.
Autocorrelation	Mathematical operation allowing you to detect periodic patterns in a surface and to qualify a surface as isotropic or not. The autocorrelation image creates a peak in the center, round or oval if the surface is isotropic or not, and secondary lobes depending on the presence or not of periodic patterns. The autocorrelation is obtained by inverse FFT by the squared module of the surface spectrum.
Bearing	Factor characterising the percentage of material in contact with a horizontal plane situated at a given depth. The bearing is characterised by the Tp parameter (or Rmr).
Binary image	Image having only two states: background or grains. A binary image is created from the Binarization (thresholding) of an image in gray levels or of a surface.
Color palette	Scale of colors used to code the altitudes on an image. The more color changes over the palette, the more depth zones near one another can be differentiated.

Cut-off	Name given to the cut wavelength when separating waviness from roughness in a filtering process. The recommended standard values are a geometrical series: 0.08 mm; 0.25 mm; 0.8 mm; 2.5 mm; 8 mm.
Filtering	Operation consisting in separating data frequencies (or wavelengths) into two parts, the first one having the long wavelengths (waviness), the other one having the short wavelengths (roughness).
Form	Components of the surface relief of long horizontal wavelengths. Form needs to be removed in order to analyze surface finish (i.e. waviness and roughness). Form can either be geometrical (sphere, cylinder, slope) or coming from a smooth material (paper, cloth). In the last case, form is calculated by a polynomial of variable degree.
Functional parameters	Surface finish parameters class characterising the functional aspect of a surface, particularly lubrication and grinding. E.g. Tp, Rk, Sbi, Sci and Svi are functional parameters.

Gaussian Filter	The Gaussian filter is a phase corrected filter, the filtering function has a Gaussian shape, i.e. with a bell-shaped curve form. The robust Gaussian filter for profiles is defined by ISO standard TS 16610-31 (2010). It is based on an iterative statistical method and the term "robust" means that the filter is capable of generating a mean line that is undisturbed by accidental or local features of a profile therefore meaning that this filter makes it possible to filter without loss at the edges. To illustrate the advantages of this, Figure 23 and Figure 24 below show examples of the different results obtained by applying either a Gaussian filter and or a robust Gaussian filter to a profile. 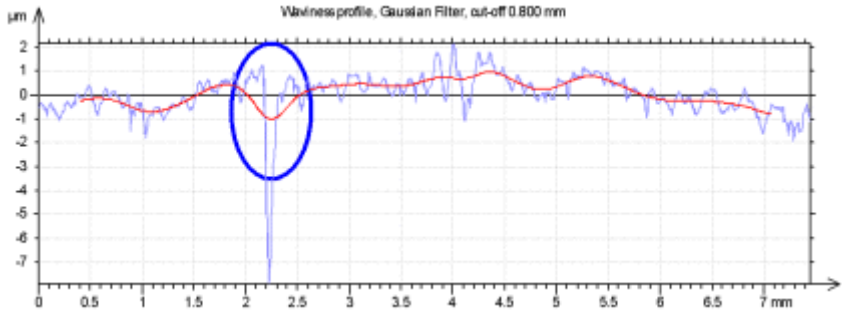 **Figure 23 Effect of a normal Gaussian filter**  **Figure 24 Effect of a robust Gaussian filter** In Figure 23 above, the mean line subsides because of the deep valley. This fault means that the roughness profile is raised in the areas surrounding the valley, and introduces an error in the roughness parameters, especially in amplitude parameters and in the bearing ratio. In the Figure 24 above, the robust mean line is faithful to the trend of the profile and provides a better description of the material. This seemed important to filter out these features in the initial low-pass waviness filter as the polishing process during the preparation of the polished enamel samples resulted in isolated scratches which were required to be removed.

Hybrid parameters	Surface finish parameters class characterising a criterion depending both of the amplitude and the spacing, such as slopes, curvatures, etc. E.g. Rq, Ssc and Sdr parameters are hybrid parameters.
Interpolation	Operation consisting in creating points between two measured points, by calculating their height from the straight line joining the two initial points (linear interpolation). This operation is also called resampling.
Isotropic / Isotropy	A surface is said isotropic when it has the same characteristics in all the directions of the measurement plane. In this case, the surface can be easily characterised using a 2D profile since this one is similar over all directions.
Kurtosis	Name given to a parameter describing the flattening of depths distribution, Rku.

Least squares method	Method enabling to look for a geometrical form that best fits the points of a measurement. The most current case is to level a profile (or a surface) by a line (or a plane) of the least squares describing best the slope of the sample. The method minimizes the square deviation between each point of the geometrical form and the points of the measurement. As shown in Figure 25 below, the Least Squares Method of leveling consists in looking for a geometrical form that best fits the points of a measurement and involves leveling a profile (or a surface) by a line (or a plane) of the least squares that best fits the slope of the sample (DigitalSurf 2013). 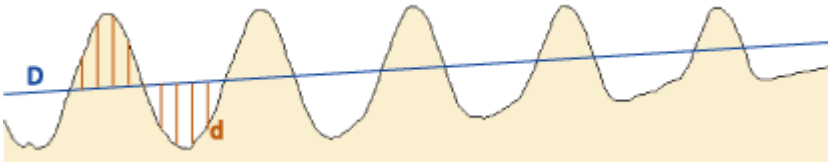 **Figure 25 Illustration of the least squares line for a profile which was used to leveling the surface using the least squares method prior to surface texture analysis** $$\Pi = d_1^2 + d_2^2 + \ldots + d_{n-1}^2 + d_n^2 = \sum_{i=1}^{n} d_i^2 = \sum_{i=1}^{n} [y_i - (a + bx_i)]^2$$ This method is recommended for surfaces with random surface texture and allows the entire surface data points to be included for the leveling, which is useful for measurements which will involve the entire surface area of the object being analysed. Once the least squares plane has been calculated then the angle between the Π plane and the horizontal is used to rotate the surface, as shown in Figure 26 below, so that it is as horizontal as possible. This allows the geometry of the surface to be kept (for example angles), however there may be smoothing effects, and the calculation can take considerable time (DigitalSurf 2013). 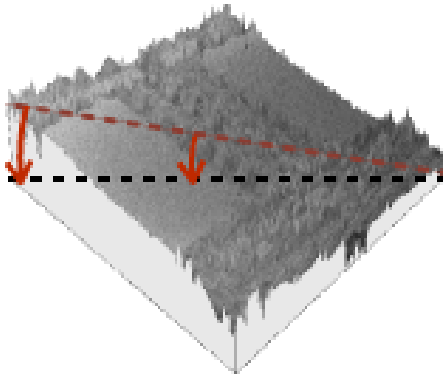 **Figure 26 Illustration demonstrating the removal of the plane from the surface using the rotation method**

Microroughness	Microroughness is the finest component of surface texture and is often responsible for the matte character of a surface. It is defined as the set of high frequencies (the smallest wavelengths) in a measurement, coming either from the sampling noise or from the microscopic relief and the structure of the material. Microroughness must be filtered before calculating the roughness parameters as defined in the different standards. In general, microroughness is discarded by band-pass filtering; using a microroughness cut-off of 2.5 µm to 25 µm. Filtering microroughness is often omitted on surfaces because of the relatively low resolution in points per profile. This resolution is highly dependent on the choice of measurement instrumentation.
Profile	Altitudes measurement along a line, often measured using a contact or laser profilometer. This type of measurement is considered as a 2D measurement, z=f(x).
Ra Arithmetical mean height	Mean profile roughness. Ra is defined as the average of the absolute values of the profile height deviations recorded within the evaluation length measured from the mean line in micrometers.
Range	The range of a profile (or of a surface) is the height between its highest peak and its deepest valley. The range can be written in microns or in digits, i.e. the number of sampling levels used to code the profile heights.
Resampling	Action of decomposing information into pieces in order to represent it as a number. A height measurement is for example resampled horizontally due to the fact that the height is not measured at regular intervals (spacing), and vertically due to the fact that the height value is converted into a number that is a multiple of a basic height increment (defining the resolution).

Resolution	Smallest variation of the value supplied by a measurement system. The resolution of a profiler is often very small (nanometers or less) but it doesn't indicate that this dimension can actually be measured by the instrument. On the contrary, a bad resolution can be the cause of a bad accuracy (for example, when the measurement range is big and the sample very small).
RMS	Root Mean Square, efficient roughness obtained by the Rq (or Sq) parameter.
Roughness	Main components of the relief containing the smallest wavelengths measured on the sample. The roughness gives indication on the nature of the material and the machining type used. Roughness is a component of surface texture varying rapidly depending on the horizontal position. Roughness is defined for example as a wavelength ranging from 20 µm to 500 µm. The wavelengths under the cut-off are kept in the roughness, the others, higher, are kept in the waviness.
Sa Arithmetical mean height	Mean surface roughness. $Sa = \frac{1}{A}\int_A \left|z(x,y)\right| dxdy$ This parameter is deprecated and shall be replaced by Sq in the future.
Sampling length	Length on which some parameter of surface finish are defined. For a filtered profile, the sampling length is equal to the cut-off length. On a raw profile, the sampling length is equal to the assessment length. Parameters are calculated on each sampling length and expressed then as the average on all the sampling lengths used. It is recommended to use 5 sampling lengths.

Series of profiles	Set of profiles measured in the same conditions (in parallel or at the same time) having the same length, stored in the same file and analyzed together in a studiable object of the series type.
Series of surfaces	A series of surfaces is a set of surfaces measured in the same conditions (in parallel measurements or measurements over time) and having the same dimensions. With this new capability, studies on the evolution of a surface in time move from a purely static ("anatomical") surface description to a more functional ("physiological") one. This type of study is suitable to analyze dynamic behaviours such as the evolution of a surface over time (accelerated ageing, dehydration, corrosion, mechanical component wear, deformation...) or the impact of a physical parameter on topography (temperature, humidity, pressure...) etc. The altitude Z is expressed according to a position X, Y over a time t or according to another parameter (pressure, temperature...): Z=f(x,y,t). The set of surfaces is considered as a single object. The surfaces are stored in the same file and are analyzed together.
Sku Kurtosis	Kurtosis of the height distribution. $Sku = \frac{1}{Sq^4}\left[\frac{1}{A}\iint_A z^4(x,y)dxdy\right]$ Fourth statistical moment, qualifying the flatness of the height distribution. Due to the big exponent used, this parameter is very sensitive to the sampling and to the noise of the measurement.

Smc Inverse areal material ratio	Height c at which a given areal material ratio p is satisfied. The height is calculated from the mean plane. 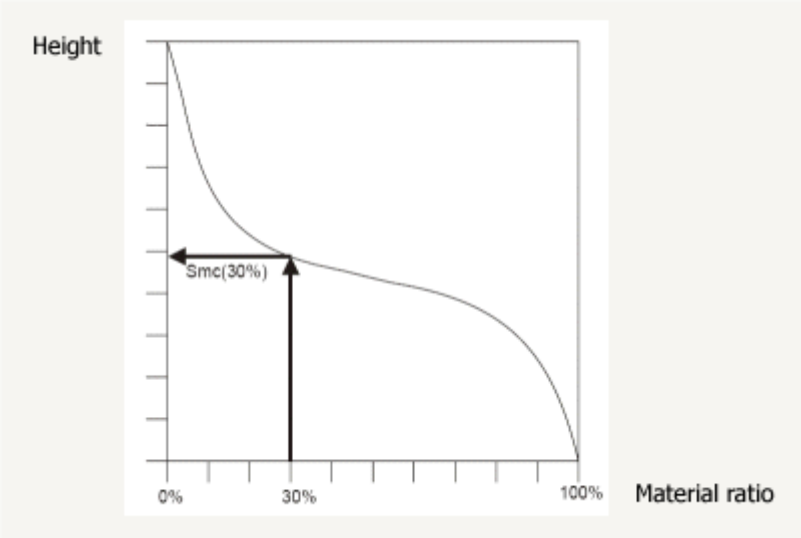
Smr Areal material ratio	Bearing area ratio at a given height. Ratio of the area of the material at a specified height c (cut level) to the evaluation area. The Smr(c) is expressed as a percentage. 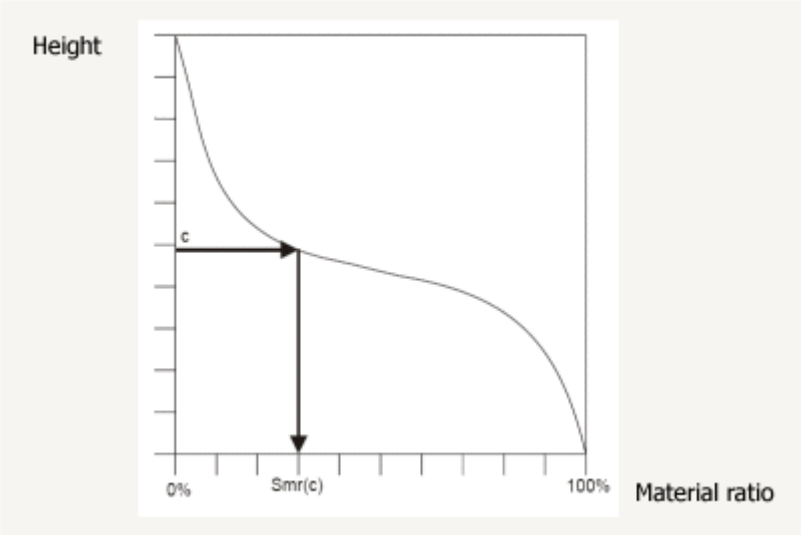 This parameter must be configured with a threshold height c (cut level) and a reference plane. For example: 3 µm under the highest peak, 1 µm above the mean, 1 µm above the threshold fixed to 20 % of Tp. The Smr parameter is included in ISO 25178 and in EUR 15178N. In the software, both parameters are calculated the same way, but with a different cut level. For both, the height c can be set from various references including the mean plane or the highest point.

Sp Maximum peak height	Height between the highest peak and the mean plane.
Spacing parameters	Surface finish parameters class characterising the spacing of motifs in the profile axis or in the surface plane. E.g. the RSm and Rq parameters are spacing parameters.
Sq Root mean square height	Standard deviation of the height distribution, or RMS surface roughness. $Sq = \sqrt{\frac{1}{A}\iint_A z^2(x,y)dxdy}$ Computes the standard deviation for the amplitudes of the surface (RMS).
Ssk Skewness	Skewness of the height distribution. $Ssk = \frac{1}{Sq^3}\left[\frac{1}{A}\iint_A z^3(x,y)dxdy\right]$ Third statistical moment, qualifying the symmetry of the height distribution. A negative Ssk indicates that the surface is composed with principally one plateau and deep and fine valleys. In this case, the distribution is sloping to the top. A positive Ssk indicates a surface with lots of peaks on a plane. The distribution is sloping to the bottom. Due to the big exponent used, this parameter is very sensitive to the sampling and to the noise of the measurement.
Surface	A real surface is the “surface limiting the body and separating it from the surrounding medium” and a measured surface is the “profile that results from the intersection of the real surface by a specified plane” ISO 4287 (1997) Thus the output from surface measurement is altitude measurements according to a Cartesian matrix z = f(x,y) made by successive measurement of parallel profiles (scanning) or by measurement using a camera iterating the vertical position of the objective.
Sv Maximum pit height	Depth between the mean plane and the deepest valley.

Sxp, Extreme peak height	Difference in height between q% and p% material ratio. This parameter must be configured with two thresholds entered in %. Sxp = Smc (q%) - Smc (p%) 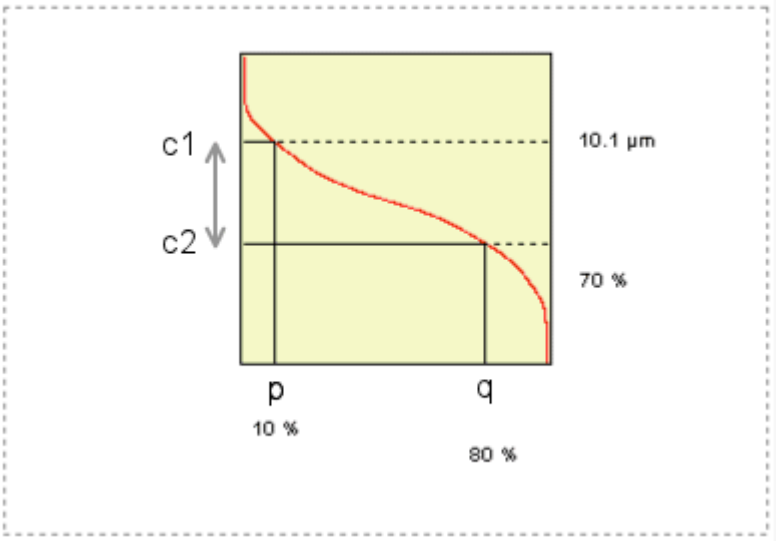
Sz Maximum height	Height between the highest peak and the deepest valley. The definition of the ISO 25178 Sz parameter (International Organisation of Standardization 2010) is different from the definition of the (EUR 15178N) Sz parameter. The value of the (EUR 15178N) Sz parameter is always smaller than the value of the (ISO 25178) Sz parameter.
Waviness	Waviness is a surface texture component composed of the long wavelengths measured on a sample. Waviness is for example defined as wavelengths ranging from 0.5 to 2.5 mm when calculating the W parameter and is sometimes derived from a defect in the tool used to form the piece (vibration, step of the tool etc.). The wavelengths above the cut-off are kept in the waviness whereas the others, smaller, are kept in the roughness, depending on the horizontal position.

Bibliography

Al-Omiri, M. K., Lamey, P. J. & Clifford, T. 2006. Impact Of Tooth Wear On Daily Living. *The International Journal Of Prosthodontics*, 19, 601- 615.

Attin, T. 2006. Methods For Assessment Of Dental Erosion. *Monographs In Oral Science*, 20, 152-172.

Austin, R. 2011. The Role Of Fluoride On Erosion, Attrition And Abrasion Of Human Enamel And Dentine In Vitro. Phd, King's College London, University Of London.

Bartlett, D., Ganss, C. & Lussi, A. 2008. Basic Erosive Wear Examination (Bewe): A New Scoring System For Scientific And Clinical Needs. *Clinical Oral Investigations*, 12, 65-68.

Bartlett, D. W., Phillips, K. M. & Smith, B. G. N. 1999. A Difference Of Perspective - The North American And European Interpretations Of Tooth Wear. *International Journal Of Prosthodontics*, 12, 401-408.

Bartlett, D. W. & Smith, B. G. N. 2000. Definition, Classification And Clinical Assessment Of Attrition, Erosion And Abrasion Of Enamel And Dentine. In: Addy, M., Embery, G., Edgar, W. M. & Orchardson, R. (Eds.) Tooth Wear And Sensitivity - Clinical Advances In Restorative Dentistry. London: Martin Dunitz.

Bell, S. 2010. A Beginner's Guide To Uncertainty Of Measurement Npl Good Practice Guide No 11, National Physical Laboratory.

Berkovitz, B. K. B. H. G. R. M. B. J. 2009. Oral Anatomy, Histology And Embryology, Edinburgh; New York, Mosby/Elsevier.

Bomfim, D. I. 2010. Quality Of Life Of Patients With Different Levels Of Tooth Wear. Master In Science, Eastman Dental Institute At The University Of London.

Christiansen, S. & De Chiffre, L. 1997. Topographic Characterization Of Progressive Wear On Deep Drawing Dies. *Tribology Transactions*, 40, 346-352.

D'agostino, R. 1986. Tests For Normal Distribution. In: D'agostino, R. & Stephens, M. (Eds.) Goodness-Of-Fit Techniques. Macel Dekker.

Digitalsurf 2013. Mountainsmap® Suface Texture Analysis Software User Manual. Availible From Http://Www.Digitalsurf.Fr/En/Usermanual.Html

Dixon, B., Sharif, M., Ahmed, F., Smith, A., Seymour, D. & Brunton, P. 2012. Evaluation Of The Basic Erosive Wear Examination (Bewe) For Use In General Dental Practice. *British Dental Journal*, 213–217.

Duschner, H., Gotz, H., Walker, H. & Lussi, A. 2000. Structural Changes Of Acid Etched Enamel Examined Under Confocal Laser Scanning Microscope. In: Addy, M., Embery, G. & Orchardson, R. (Eds.) Tooth Wear And Sensitivity. London: Martin Dunitz.

Featherstone, J. D. & Lussi, A. 2006. Understanding The Chemistry Of Dental Erosion. *Monographs In Oral Science*, 20, 66-76.

Field, J., Waterhouse, P. & German, M. 2010. Quantifying And Qualifying Surface Changes On Dental Hard Tissues In Vitro. *Journal Of Dentistry*, 38, 182-190.

Graphpad Software. 2013. Graphpad Statistics Guide [Online]. Available From : Http://Www.Graphpad.Com/Guides/Prism/6/Statistics/Index.Htm?Stat_---_Principles_Of_Statistics_-.Htm 2013].

Heurich, E., Beyer, M., Jandt, K. D., Reichert, J., Herold, V., Schnabelrauch, M. & Sigusch, B. W. 2010. Quantification Of Dental Erosion—A Comparison Of Stylus Profilometry And Confocal Laser Scanning Microscopy (CLSM). *Dental Materials*, 26, 326-336.

International Organisation Of Standardization 1996. Iso 3274 Geometrical Product Specifications (Gps) – Surface Texture: Profile Method – Nominal Characteristics Of Contact (Stylus) Instruments. International Organisation Of Standardization.

International Organisation Of Standardization 1997. Iso 4287. Geometrical Product Specifications (Gps) – Surface Texture: Profile Method – Terms, Definitions And Surface Texture Parameters International Organisation Of Standardization.

International Organisation Of Standardization 2000. Iso 5436-1. Geometrical Product Specifications (Gps) - Surface Texture: Profile Method; Measurement Standards - Part 1: Material Measures.

International Organisation Of Standardization 2010a. Iso 25178. Geometric Product Specifications (Gps) – Surface Texture: Areal.

International Organisation Of Standardization 2010b. Iso/Ts 16610-31. Geometrical Product Specifications (Gps) -- Filtration -- Part 31: Robust Profile Filters: Gaussian Regression Filters.

Isecke, B., Schütze, M. & Strehblow, H.-H. 2011. Corrosion. In: Czichos, H., Saito, T. & Smith, L. (Eds.) Springer Handbook Of Metrology And Testing. Springer Berlin Heidelberg.

Jones, S. B., Chew, H. P., Zakian, C. M., Ellwood, R. P., Davies, M. & West, N. X. Quantifying Effectiveness Of Fluoride To Reduce

Erosion Of Natural Surface And Polished Enamel In Situ. 60th Orca Congress. July 3-6, 2013,, 2013 Liverpool, Uk. 433-531.
Kreulen, C., Van't Spijker, A., Rodriguez, J., Bronkhorst, E., Creugers, N. & Bartlett, D. 2010. Systematic Review Of The Prevalence Of Tooth Wear In Children And Adolescents. *Caries Research*, 44, 151-159.
Larsen, M. J. 1990. Chemical Events During Tooth Dissolution. Journal Of Dental Research, 69 Spec No, 575-580.
Las Casas, E. B., Bastos, F. S., Godoy, G. C. D. & Buono, V. T. L. 2008. Enamel Wear And Surface Roughness Characterization Using 3d Profilometry. *Tribology International*, 41, 1232-1236.
Leach, R. K. 2010a. Fundamental Principles Of Engineering Nanometrology [Online]. Oxford; Amsterdam: William Andrew ; Elsevier Science. Available: Http://Www.Sciencedirect.Com/Science/Book/9780080964546.
Leach, R. K. 2010b. Surface Topography Characterisation. In: Fundamental Principles Of Engineering Nanometrology. Oxford; Amsterdam: William Andrew ; Elsevier Science.
Leach, R. K. 2010c. Surface Topography Measurement Instrumentation. In: Fundamental Principles Of Engineering Nanometrology. Oxford; Amsterdam: William Andrew ; Elsevier Science.
Lussi, A. 2011. Dental Erosion Diagnosis, Risk Assessment, Prevention, Treatment, London; Quintessence Publ.
Lussi, A., Schlueter, N., Rakhmatullina, E. & Ganss, C. 2011. Dental Erosion–An Overview With Emphasis On Chemical And Histopathological Aspects. *Caries Research*, 45, 2-12.
Nowicki, B. 1985. Multiparameter Representation Of Surface Roughness. *Wea*r, 102, 161-176.
O'sullivan, E. A. & Milosevic, A. 2007. Diagnosis, Prevention And Management Of Dental Erosion. Faculty Of Dental Surgery Of The Royal College Of Surgeons Of England.
Oxford English Dictionary. 2010. "Surface, N." [Online]. Oxford University Press. Available: Http://Www.Oed.Com/Viewdictionaryentry/Entry/194886 [Accessed November 2010.
Rakhmatullina, E., Bossen, A., Höschele, C., Wang, X., Beyeler, B., Meier, C. & Lussi, A. 2011. Application Of The Specular And Diffuse Reflection Analysis For In Vitro Diagnostics Of Dental Erosion: Correlation With Enamel Softening, Roughness, And

Calcium Release. *Journal Of Biomedical Optics*, 16, 107002-107015.

Reid, D. J. & Ferrell, R. J. 2006. The Relationship Between Number Of Striae Of Retzius And Their Periodicity In Imbricational Enamel Formation. Journal Of Human Evolution, 50, 195-202.

Risnes, S. 1986. Enamel Apposition Rate And The Prism Periodicity In Human Teeth. *European Journal Of Oral Sciences*, 94, 394-404.

Rodriguez, J. M., Austin, R. S. & Bartlett, D. W. 2012. In Vivo Measurements Of Tooth Wear Over 12 Months. *Caries Research*, 46, 9-15.

Schlueter, N., Hara, A., Shellis, R. & Ganss, C. 2011. Methods For The Measurement And Characterization Of Erosion In Enamel And Dentine. *Caries Research*, 45, 13-23.

Seah, M. & De Chiffre, L. 2011. Surface And Interface Charaterisation. In: Czichos, H., Saito, T. & Smith, L. M. (Eds.) Springer Handbook Of Metrology And Testing. Berlin: Springer Berlin.

Simmer, J. P., Papagerakis, P., Smith, C. E., Fisher, D. C., Rountrey, A. N., Zheng, L. & Hu, J. C.-C. 2010. Regulation Of Dental Enamel Shape And Hardness. *Journal Of Dental Research*, 89, 1024-1038.

The Information Centre For Health And Social Care 2011. Adult Dental Health Survey 2009.

Van't Spijker, A., Rodriguez, J. M., Kreulen, C. M., Bartlett, D. W. & Creugers, N. H. 2009. Prevalence Of Tooth Wear In Adults. *International Journal Of Prosthodontics*, 22, 35-42.

World Health Organisation 1992. Application Of The International Classification Of Diseases To Dentistry And Stomatology, Icd-Da, Geneva.

Young, A. & Tenuta, L. M. A. 2011. Initial Erosion Models. *Caries Research*, 45(Suppl 1), 33-42.

Zhang, X., Anderson, P., Dowker, S. & Elliott, J. 2000. Optical Profilometric Study Of Changes In Surface Roughness Of Enamel During In Vitro Demineralization. *Caries Research*, 34, 164-174.